Born-Oppenheimer Approximation for the XYZ Mesons

Eric Braaten, Christian Langmack, and D. Hudson Smith

Department of Physics,
The Ohio State University,
Columbus, OH 43210, USA

(Dated: February 4, 2014)

arXiv:1402.0438v1 [hep-ph] 3 Feb 2014

Abstract

Many of the XYZ mesons discovered in the last decade can be identified as bound states in Born-Oppenheimer (B-O) potentials for a heavy quark and antiquark. They include quarkonium hybrids, which are bound states in excited flavor-singlet B-O potentials, and quarkonium tetraquarks, which are bound states in flavor-nonsinglet B-O potentials. We present simple parameterizations of the deepest flavor-singlet B-O potentials. We infer the deepest flavor-nonsinglet B-O potentials from lattice QCD calculations of static adjoint mesons. Selection rules for hadronic transitions are used to identify XYZ mesons that are candidates for ground-state energy levels in the B-O potentials for charmonium hybrids and tetraquarks. The energies of the lowest-energy charmonium hybrids are predicted by using the results of lattice QCD calculations to calculate the energy splittings between the ground states of different B-O potentials and using the Schroedinger equation to determine the splittings between energy levels within a B-O potential.

PACS numbers: 14.40.Pq,14.40.Rt,31.30.-i,13.25.Gv

Keywords: Quarkonium, hybrid mesons, tetraquark mesons, exotic mesons, Born-Oppenheimer approximation, hadronic transitions, selections rules.

I. INTRODUCTION

The XYZ mesons are unexpected mesons discovered during the last decade that contain a heavy quark-antiquark pair and are above the open-heavy-flavor threshold. Some of the more surprising of these XYZ mesons are

- $X(3872)$, discovered by the Belle Collaboration in 2003 [1]. It has comparable branching fractions into $J/\psi\,\rho$ and $J/\psi\,\omega$, implying a severe violation of isospin symmetry.
- $Y(4260)$, discovered by the BaBar Collaboration in 2005 [2]. It has J^{PC} quantum numbers 1^{--}, but it is produced very weakly in e^+e^- annihilation.
- $Y(4140)$, discovered by the CDF Collaboration in 2009 [3]. It decays into $J/\psi\,\phi$, which suggests that it might be a tetraquark meson with constituents $c\bar{c}s\bar{s}$.
- $Z_b^+(10610)$ and $Z_b^+(10650)$, discovered by the Belle Collaboration in 2011 [4]. They both decay into $\Upsilon\,\pi^+$, which implies that they must be tetraquark mesons with constituents $b\bar{b}u\bar{d}$.
- $Z_c^+(3900)$, discovered by the BESIII Collaboration in 2013 [5]. It decays into $J/\psi\,\pi^+$, which implies that it must be a tetraquark meson with constituents $c\bar{c}u\bar{d}$.

An updated list of the XYZ mesons as of August 2013 was given in Ref. [6]. In the $c\bar{c}$ meson sector, the list consisted of 15 neutral and 4 charged states. In the $b\bar{b}$ meson sector, the list consisted of 1 neutral and 2 charged states.

More than a decade has elapsed since the discovery of the $X(3872)$, and no compelling explanation for the pattern of XYZ mesons has emerged. Simple constituent models for the XYZ mesons can be classified according to their constituents and how they are clustered within the meson. Those that have been proposed include

- **conventional quarkonium**, which consists of a color-singlet heavy quark-antiquark pair: $(Q\bar{Q})_1$,
- **quarkonium hybrid meson**, which consists of a color-octet $Q\bar{Q}$ pair to which a gluonic excitation is bound: $(Q\bar{Q})_8 + g$,
- **compact tetraquark** [7], which consists of a $Q\bar{Q}$ pair and a light quark q and antiquark $\bar{q}$ bound by inter-quark potentials into a color singlet: $(Q\bar{Q}q\bar{q})_1$,
- **meson molecule** [8], which consists of color-singlet $Q\bar{q}$ and $\bar{Q}q$ mesons bound by hadronic interactions: $(Q\bar{q})_1 + (\bar{Q}q)_1$,
- **diquark-onium** [9], which consists of a color-antitriplet Qq diquark and a color-triplet $\bar{Q}\bar{q}$ diquark bound by the QCD color force: $(Qq)_{\bar{3}} + (\bar{Q}\bar{q})_3$,
- **hadro-quarkonium** [10], which consists of a color-singlet $Q\bar{Q}$ pair to which a color-singlet light-quark pair is bound by residual QCD forces: $(Q\bar{Q})_1 + (q\bar{q})_1$. An essentially equivalent model is a quarkonium and a light meson bound by hadronic interactions.
- **quarkonium adjoint meson** [11], which consists of a color-octet $Q\bar{Q}$ pair to which a light quark-antiquark pair is bound: $(Q\bar{Q})_8 + (q\bar{q})_8$.

All of these are possible models for neutral XYZ mesons. The last five are possible models for charged XYZ mesons. None of these models has proven to be very predictive for the pattern of XYZ mesons. They are all essentially phenomenological models whose only connection with the fundamental field theory QCD is that they use degrees of freedom from QCD. It would be desirable to have a single theoretical framework based firmly on QCD that describes all the XYZ mesons. One possibility for such a framework is the Born-Oppenheimer (B-O) approximation.

The B-O approximation is used in atomic and molecular physics to understand the binding of atoms into molecules [12]. It exploits the large ratio of the time scale for the motion of the atomic nuclei to that for the electrons, which is a consequence of the large ratio of the mass of a nucleus to that of the electron. The electrons respond almost instantaneously to the motion of the nuclei. Their instantaneous configuration is determined by the positions of the nuclei, which can be approximated by static sources for the electric field. The energy of the electrons combined with the repulsive Coulomb energy of the nuclei defines a Born-Oppenheimer (B-O) potential. The B-O approximation to the energy levels of the molecule are the energy eigenvalues of the Schroedinger equation in that potential.

The B-O approximation for $Q\bar{Q}$ mesons in QCD was developed by Juge, Kuti, and Morningstar [13]. It exploits the large ratio of the time scale for the motion of the Q and $\bar{Q}$ to that for the evolution of gluon fields, which is a consequence of the large ratio of the heavy-quark mass m_Q to the nonperturbative momentum scale $\Lambda_{\rm QCD}$ associated with the gluon field. The gluon field responds almost instantaneously to the motion of the Q and $\bar{Q}$. Its instantaneous configuration is determined by the positions of the Q and $\bar{Q}$, which can be approximated by static color sources. The energy of the gluon field defines a B-O potential $V_\Gamma(r)$ that depends on the separation r of the Q and $\bar{Q}$ and on the quantum numbers Γ for the gluon field in the presence of static Q and $\bar{Q}$ sources. The motion of the Q and $\bar{Q}$ can be described by the Schroedinger equation with potential $V_\Gamma(r)$. In the B-O approximation, $Q\bar{Q}$ mesons are energy levels of the Schroedinger equation in the B-O potentials. The energy levels in the ground-state potential are conventional quarkonia. The energy levels in the excited-state potentials are quarkonium hybrids.

Juge, Kuti, and Morningstar calculated many of the B-O potentials using quenched lattice QCD, in which light-quark loops are omitted [13]. They calculated the spectrum of bottomonium hybrids by solving the Schroedinger equation in the B-O potentials. They also calculated some of the bottomonium hybrid energies using lattice NRQCD. The quantitative agreement between the predictions of the B-O approximation and lattice NRQCD provided convincing evidence for the existence of quarkonium hybrids in the hadron spectrum of QCD.

For QCD with light quarks, the B-O potentials can be defined as the energies of stationary configurations of the gluon and light-quark fields whose flavor quantum numbers are singlet in the presence of static Q and $\bar{Q}$ sources. In Ref. [11], it was pointed out that B-O potentials can also be defined by the energies of stationary configurations of light-quark and gluon fields that have flavor-nonsinglet quantum numbers. The energy levels of a $Q\bar{Q}$ pair in such a flavor-nonsinglet potential are quarkonium tetraquarks. Several of the simple constituent models for quarkonium tetraquarks itemized above can be identified with specific regions of the Born-Oppenheimer wavefunction for the $Q\bar{Q}$ pair. When the separation of the $Q\bar{Q}$ pair is much smaller than the spatial extent of the light-quark and gluon fields, the system resembles a quarkonium adjoint meson $(Q\bar{Q})_8+(q\bar{q})_8$. When the Q and $\bar{Q}$ are well separated, the system resembles a meson molecule $(Q\bar{q})_1+(\bar{Q}q)_1$ if the light quark is localized near the

State	M (MeV)	Γ (MeV)	J^{PC}	Decay modes	1st observation
$X(3823)$	3823.1±1.9	< 24	$?^{?-}$	$\chi_{c1}\gamma$	Belle 2013
$X(3872)$	3871.68±0.17	< 1.2	1^{++}	$J/\psi\,\pi^+\pi^-$, $J/\psi\,\pi^+\pi^-\pi^0$	Belle 2003
				$D^0\bar{D}^0\pi^0$, $D^0\bar{D}^0\gamma$	
				$J/\psi\,\gamma$, $\psi(2S)\,\gamma$	
$X(3915)$	3917.5 ± 1.9	20±5	0^{++}	$J/\psi\,\omega$, $(\gamma\gamma)$	Belle 2004
$\chi_{c2}(2P)$	3927.2 ± 2.6	24±6	2^{++}	$D\bar{D}$, $(\gamma\gamma)$	Belle 2005
$X(3940)$	3942^{+9}_{-8}	37^{+27}_{-17}	$?^{?+}$	$D^*\bar{D}$, $D\bar{D}^*$	Belle 2007
$G(3900)$	3943 ± 21	52±11	1^{--}	$D\bar{D}$, (e^+e^-)	*BABAR* 2007
$Y(4008)$	$4008^{+121}_{-\ 49}$	226±97	1^{--}	$J/\psi\,\pi^+\pi^-$, (e^+e^-)	Belle 2007
$Y(4140)$	4144.5 ± 2.6	$15^{+11}_{-\ 7}$	$?^{?+}$	$J/\psi\,\phi$	CDF 2009
$X(4160)$	4156^{+29}_{-25}	139^{+113}_{-65}	$?^{?+}$	$D^*\bar{D}^*$	Belle 2007
$Y(4220)$	4216 ± 7	39 ± 17	1^{--}	$h_c(1P)\,\pi^+\pi^-$, (e^+e^-)	BESIII 2013
$Y(4260)$	4263^{+8}_{-9}	95±14	1^{--}	$J/\psi\,\pi^+\pi^-$, $J/\psi\,\pi^0\pi^0$	*BABAR* 2005
				$Z_c(3900)\,\pi$, (e^+e^-)	
$Y(4274)$	$4274.4^{+8.4}_{-6.7}$	32^{+22}_{-15}	$?^{?+}$	$J/\psi\,\phi$	CDF 2010
$X(4350)$	$4350.6^{+4.6}_{-5.1}$	$13.3^{+18.4}_{-10.0}$	$0/2^{++}$	$J/\psi\,\phi$, $(\gamma\gamma)$	Belle 2009
$Y(4360)$	4361 ± 13	74±18	1^{--}	$\psi(2S)\,\pi^+\pi^-$, (e^+e^-)	*BABAR* 2007
$X(4630)$	$4634^{+\ 9}_{-11}$	92^{+41}_{-32}	1^{--}	$\Lambda_c^+\Lambda_c^-$, (e^+e^-)	Belle 2007
$Y(4660)$	4664±12	48±15	1^{--}	$\psi(2S)\,\pi^+\pi^-$, (e^+e^-)	Belle 2007

TABLE I: Neutral $c\bar{c}$ mesons above the $D\bar{D}$ threshold discovered since 2003. Neutral isospin partners of charged $c\bar{c}$ mesons are not listed. The "decay modes" in parenthesis, (e^+e^-) and $(\gamma\gamma)$, are actually production channels.

$\bar{Q}$ and it resembles diquark-onium $(Qq)_{\bar{3}} + (\bar{Q}\bar{q})_3$ if the light quark is localized near the Q.

In this paper, we apply the B-O approximation for quarkonium hybrids and tetraquarks to the XYZ mesons. In Section II, we list the XYZ mesons that have been observed so far. In Section III, we discuss the B-O potentials for quarkonium hybrids and tetraquarks. We present accurate parametrizations of the deepest hybrid B-O potentials, and we infer the deepest tetraquark B-O potentials from lattice QCD calculations of static adjoint mesons. In Section IV, we apply the B-O approximation to quarkonium hybrid and tetraquark mesons. We derive selection rules for hadronic transitions between Born-Oppenheimer configurations and use them to identify XYZ mesons that are candidates for ground-state energy levels of charmonium hybrids and tetraquarks. In Section V, we describe lattice QCD calculations of $c\bar{c}$ and $b\bar{b}$ mesons and discuss their implications for the B-O approximation. In Section VI, we predict the lowest energy levels of charmonium hybrids by combining results from lattice QCD with energy splittings from solutions of the Schoroedinger equation in B-O potentials. The outlook for developing the B-O approximation into a systematic theory of the XYZ mesons is discussed in Section VII.

State	M (MeV)	Γ (MeV)	J^{PC}	Decay modes	1st observation
$Z_c^+(3885)$	3883.9 ± 4.5	24.8 ± 11.5	$1^{+?}$	$D^{*+}\bar{D}^0$, $D^+\bar{D}^{*0}$	BESIII 2013
$Z_c^+(3900)$	3898 ± 5	51 ± 19	$?^{?-}$	$J/\psi\,\pi^+$	BESIII 2013
$Z_c^+(4020)$	4022.9 ± 2.8	7.9 ± 3.7	$?^{?-}$	$h_c(1P)\,\pi^+$, $D^{*+}\bar{D}^{*0}$	BESIII 2013
$Z_1^+(4050)$	4051^{+24}_{-43}	82^{+51}_{-55}	$?^{?+}$	$\chi_{c1}(1P)\,\pi^+$	Belle 2008
$Z_2^+(4250)$	$4248^{+185}_{-\ 45}$	$177^{+321}_{-\ 72}$	$?^{?+}$	$\chi_{c1}(1P)\,\pi^+$	Belle 2008
$Z^+(4430)$	4443^{+24}_{-18}	$107^{+113}_{-\ 71}$	1^{+-}	$\psi(2S)\,\pi^+$	Belle 2007

TABLE II: Positively charged $c\bar{c}$ mesons. The C in J^{PC} is that of a neutral isospin partner.

II. *XYZ* MESONS

Lists of the XYZ mesons in both the $c\bar{c}$ and $b\bar{b}$ sectors, with references to all the experiments, are given in Ref. [6]. The list of new neutral $c\bar{c}$ mesons above the $D\bar{D}$ threshold consists of 15 states. The most essential information in that list, including the mass, width, J^{PC} quantum numbers, and decay modes, is repeated in Table I. This list includes an additional state labelled $Y(4220)$. The $Y(4220)$ is a narrow structure in the cross section for e^+e^- annihilation into $h_c(1P)\,\pi^+\pi^-$ that was recently observed by the BESIII collaboration [14]. Table I also includes the additional decay mode $Z_c(3900)\,\pi$ of the $Y(4260)$ observed by the Belle Collaboration [15].

The list of the charged $c\bar{c}$ mesons in Ref. [6] consists of 4 states. The most essential information in that list is repeated in Table II. The C in J^{PC} is the charge conjugation quantum number of the neutral isospin partner. It coincides with $-G$, the negative of the G-parity quantum number for the isospin triplet. Table II gives the J^P quantum numbers of the $Z^+(4430)$, which were recently determined to be 1^+ by the Belle Collaboration [16]. Table II includes two additional states that were observed more recently by the BESIII collaboration. The $Z_c^+(3885)$ was observed in the decay channels $D^{*+}\bar{D}^0$ and $D^+\bar{D}^{*0}$, and its J^P quantum numbers are favored to be 1^+ [17]. The $Z_c^+(4020)$ was observed in the decay channel $h_c(1P)\,\pi^+$ [18]. The $Z_c^+(4025)$ was subsequently observed in the decay channel $(D^*\bar{D}^*)^+$ with a mass consistent with that of $Z_c^+(4020)$ but with a larger width [19]. In Table II, they are assumed to be the same state. The neutral isospin partner $Z_c^0(3900)$ of the $Z_c^+(3900)$ has been observed [20], but it is not included in the list of neutral mesons in Table I.

The decay modes of the $c\bar{c}$ mesons listed in Tables I and II are of four kinds:

- a hadronic decay into a pair of charm mesons, such as $D\bar{D}$, or a pair of charm baryons, such as $\Lambda_c^+\Lambda_c^-$,
- a hadronic transition to a lighter $c\bar{c}$ meson through the emission of light hadrons, such as a single vector meson ω or ϕ, a single pion, or a pair of pions,
- an electromagnetic transition to a lighter $c\bar{c}$ meson through the emission of a photon,
- an electromagnetic annihilation "decay mode" (e^+e^-) or $(\gamma\gamma)$, in which the parentheses indicate that it has actually been observed as a production channel. They provide strong constraints on the J^{PC} quantum numbers: (e^+e^-) requires 1^{--} and $(\gamma\gamma)$ requires either 0^{++} or 2^{++}.

State	M (MeV)	Γ (MeV)	J^{PC}	Decay modes	1st observation
$Y_b(10890)$	10888.4±3.0	$30.7^{+8.9}_{-7.7}$	1^{--}	$\Upsilon(nS)\,\pi^+\pi^-$, (e^+e^-)	Belle 2010
$Z_b^+(10610)$	10607.2±2.0	18.4±2.4	1^{+-}	$\Upsilon(nS)\,\pi^+$, $h_b(nP)\,\pi^+$	Belle 2011
				$\bar{B}^{*0}B^+$, $\bar{B}^0B^{*+}$	
$Z_b^+(10650)$	10652.2±1.5	11.5±2.2	1^{+-}	$\Upsilon(nS)\,\pi^+$, $h_b(nP)\,\pi^+$	Belle 2011
				$\bar{B}^{*0}B^{*+}$	

TABLE III: Neutral and positively charged $b\bar{b}$ mesons above the $B\bar{B}$ threshold discovered since 2003. Neutral isospin partners of charged $b\bar{b}$ mesons are not listed. For a charged $b\bar{b}$ meson, the C in J^{PC} is that of the neutral isospin partner.

The list of new $b\bar{b}$ mesons above the $B\bar{B}$ threshold in Ref. [6] consists of 1 neutral and 2 charged states. The most essential information in that list is repeated in Table III. Table III includes additional decay modes of the $Z_b^+(10610)$ and $Z_b^+(10650)$ into pairs of bottom mesons [21]. The neutral isospin partner $Z_b^0(10610)$ of the $Z_b^+(10610)$ has been observed [22], but it is not included in the list of neutral mesons in Table III.

A theoretical framework for the XYZ mesons should explain the pattern of all the observed mesons, including their masses, widths, quantum numbers, and decay modes. It should also predict other XYZ mesons that await discovery. The theoretical framework should be based as closely as possible on the fundamental field theory QCD. It should involve the fundamental degrees of freedom of QCD, which are quark and gluon fields, and any interactions should be derivable from the fundamental QCD interactions, which are mediated by the exchange of gluons. The B-O approximation provides such a theoretical framework.

III. BORN-OPPENHEIMER POTENTIALS

In this section, we discuss the behavior of the various Born-Oppenheimer (B-O) potentials for $Q\bar{Q}$ mesons. We give simple analytic approximations for the deepest of the hybrid potentials that have been calculated using lattice QCD. We also infer the deepest of the tetraquark potentials from lattice QCD calculations of adjoint mesons.

A. Definitions of Born-Oppenheimer potentials

In QCD without light quarks, the ground-state B-O potential $V_{\Sigma_g^+}(r)$ can be defined as the minimal energy for configurations of the gluon field in the presence of Q and $\bar{Q}$ sources separated by a distance r. An excited B-O potential $V_\Gamma(r)$ can be defined as the minimal energy for configurations of the gluon field with quantum numbers specified by Γ, provided $V_\Gamma(r)$ is smaller than the sum of $V_{\Sigma_g^+}(r)$ and the mass of a glueball with the appropriate quantum numbers. Otherwise, the minimal-energy configuration is the Σ_g^+ gluon configuration accompanied by a zero-momentum glueball. A potential $V_\Gamma(r)$ that is larger than the sum of $V_{\Sigma_g^+}(r)$ and the mass of the glueball may still be well-defined as the energy of a stationary gluon configuration that is localized near the line connecting the Q and $\bar{Q}$. A prescription for the potential might involve calculating the energies of excited configurations

of the gluon field with quantum numbers Γ in the presence of Q and $\bar{Q}$ sources separated by r, and identifying the potential $V_\Gamma(r)$ as the energy of one of the excited configurations.

In QCD with light quarks, there are additional complications in the definitions of the excited flavor-singlet B-O potentials. For small r, the minimal-energy configuration is the Σ_g^+ configuration accompanied by either two or three pions, depending on the quantum numbers of Γ. For large r, the minimal-energy configuration consists of two *static mesons*, which are configurations of the light-quark and gluon fields bound to a static Q or $\bar{Q}$ source. One of the static mesons has the flavor of a light antiquark $\bar{q}$ and is localized near the Q source, while the other has the flavor of a light quark q land is localized near the $\bar{Q}$ source. The energy of such a configuration defines a B-O potential that approaches a constant as $r \to \infty$. As r decreases, the extrapolation of this potential crosses the extrapolations of the Σ_g^+ and other potentials. However there are actually avoided crossings between pairs of potentials that share the same quantum numbers Γ. If r is not too close to an avoided crossing, a B-O potential $V_\Gamma(r)$ may still be well-defined as the energy of a stationary configuration of the gluon and light-quark fields. A prescription for the potential might involve calculating the energies of excited configurations of gluon and light-quark fields with quantum numbers Γ in the presence of Q and $\bar{Q}$ sources separated by r, and identifying the potential $V_\Gamma(r)$ as the energy of one of the excited configurations.

Light quarks introduce an additional complication that is the key to understanding the tetraquark XYZ states. The gluon and light-quark configurations in the presence of static Q and $\bar{Q}$ sources are specified not only by the traditional quantum numbers Γ of the Born-Oppenheimer (B-O) approximation but also by light-quark flavor quantum numbers. As pointed out in Ref. [11], B-O potentials can also be defined for isospin-1 configurations of light-quark and gluon fields. They can also be defined for isospin-0 configurations and for configurations that contain a strange quark and a lighter antiquark. The energy levels in these potentials are tetraquark mesons. Thus the B-O approximation can be used to describe conventional quarkonium, quarkonium hybrids, and quarkonium tetraquarks all within a common framework. The definition of flavor-nonsinglet tetraquark potentials suffers from the same complications as the excited-state flavor-singlet B-O potentials. At large r, the minimal-energy configuration consists of two static mesons localized near the Q and $\bar{Q}$ sources. At small r, the minimal-energy configuration is the flavor-singlet Σ_g^+ potential accompanied by one or two pions, depending on the quantum numbers Γ. Thus the minimal-energy prescription is inadequate, and it is necessary to use a more complicated prescription to define the flavor-nonsinglet B-O potentials. A prescription for the potential might involve calculating the energies of excited configurations of gluon and light-quark fields with quantum numbers Γ and the appropriate flavors in the presence of Q and $\bar{Q}$ sources separated by r, and identifying the potential $V_\Gamma(r)$ as the energy of one of the excited configurations.

B. Light-field quantum numbers

The B-O potentials can be labelled by quantum numbers for the gluon and light-quark fields that are conserved in the presence of static Q and $\bar{Q}$ sources. We first consider the flavor-singlet case. Let $\boldsymbol{r}$ be the separation vector between the Q and $\bar{Q}$ sources. There are three conserved quantum numbers for the light fields in the presence of these sources:

- the eigenvalue λ of $\hat{\boldsymbol{r}} \cdot \boldsymbol{J}_{\rm light}$, where $\boldsymbol{J}_{\rm light}$ is the total angular momentum vector for the light fields. The possible values of λ are 0, ± 1, ± 2, ... We denote its absolute value

by Λ: $\Lambda = |\lambda|$.

- the eigenvalue η of $(CP)_{\rm light}$, which is the product of the charge-conjugation operator $C_{\rm light}$ for the light fields and the parity operator $P_{\rm light}$ that spacially inverts these fields through the midpoint between the Q and $\bar{Q}$ sources. The possible values of η are $+1$ and -1.

- for the case $\lambda = 0$, the eigenvalue ϵ of a reflection operator $R_{\rm light}$ that reflects the light fields through a plane containing the Q and $\bar{Q}$ sources. The possible values of ϵ are $+1$ or -1.

It is traditional to use an upper-case Greek letter to specify the integer Λ: Σ for $\Lambda = 0$, Π for $\Lambda = 1$, Δ for $\Lambda = 2$, etc. The eigenvalue $+1$ or -1 of $(CP)_{\rm light}$ is traditionally specified by a subscript g or u on the upper-case Greek letter. In the case $\lambda = 0$, the value $+1$ or -1 of ϵ is traditionally specified by a superscript $+$ or $-$ on Σ. Thus the B-O potentials are traditionally labelled by $\Gamma = \Sigma_\eta^+, \Sigma_\eta^-, \Pi_\eta, \Delta_\eta, \ldots$, where the subscript η is g or u.

The stationary configuration of gluon and light-quark fields associated with the quantum numbers $\lambda = 0$, η, and ϵ can be represented by the ket $|0, \eta, \epsilon\,; \boldsymbol{r}\rangle$. It is an eigenstate of $(CP)_{\rm light}$ and $P_{\rm light}$ with eigenvalues η and ϵ, respectively. The stationary configuration of gluon and light-quark fields associated with the quantum numbers $\lambda \neq 0$ and η can be represented by the ket $|\lambda, \eta; \boldsymbol{r}\rangle$. The reflection operator $R_{\rm light}$ can be expressed as the product of the parity operator $P_{\rm light}$ and a rotation by angle π around the axis perpendicular to the reflection plane and passing through the midpoint between the Q and $\bar{Q}$ sources. It maps a configuration $|\lambda, \eta; \boldsymbol{r}\rangle$ with $|\lambda| \geq 1$ into $(-1)^\lambda |-\lambda, \eta; \boldsymbol{r}\rangle$. The reflection symmetry guarantees that the configurations $|\Lambda, \eta; \boldsymbol{r}\rangle$ and $|-\Lambda, \eta; \boldsymbol{r}\rangle$ have the same energies. We can form linear combinations of these states that are eigenstates of $R_{\rm light}$:

$$\big|\Lambda, \eta, \epsilon\,; \boldsymbol{r}\big\rangle \equiv \frac{1}{\sqrt{2}}\Big(\big|\Lambda, \eta; \boldsymbol{r}\big\rangle + \epsilon\,\big|-\Lambda, \eta; \boldsymbol{r}\big\rangle\Big). \tag{1}$$

They are eigenstates of $|\hat{\boldsymbol{r}} \cdot \boldsymbol{J}_{\rm light}|$, $(CP)_{\rm light}$, and $R_{\rm light}$ with eigenvalues Λ, η, and ϵ, where ϵ is $+1$ or -1. They are also eigenstates of $P_{\rm light}$ with eigenvalue $\epsilon\,(-1)^\Lambda$. Thus the stationary light-field configurations can be labeled by the quantum numbers Λ, η, and ϵ or alternatively by $\Gamma = \Sigma_\eta^\epsilon, \Pi_\eta^\epsilon, \Delta_\eta^\epsilon, \ldots$, where the subscript η is g or u and the superscript ϵ is $+$ or $-$.

For quarkonium tetraquark mesons, the stationary configurations of the gluon and light-quark fields also have flavor quantum numbers. The flavor quantum numbers can be identified by specifying the light quark and antiquark: $q_1\bar{q}_2$, where $q_1, q_2 = u, d, s$. We proceed to discuss the conserved quantum numbers for light-field configurations with flavor quantum numbers $q_1\bar{q}_2$ in the presence of static Q and $\bar{Q}$ sources. The eigenvalue λ of $\hat{\boldsymbol{r}} \cdot \boldsymbol{J}_{\rm light}$ remains conserved. If q_1 and q_2 are distinct flavors, $C_{\rm light}$ changes the flavor from $q_1\bar{q}_2$ to $q_2\bar{q}_1$. Thus $(CP)_{\rm light}$ followed by the flavor interchange $q_1 \leftrightarrow q_2$ is a symmetry of the light-field configurations. Its quantum number η is conserved. If $\lambda = 0$, the reflection quantum number ϵ is also conserved. Thus the stationary field configurations can be labelled by $q_1\bar{q}_2$, λ, η, and also ϵ if $\lambda = 0$. Alternatively, for $|\lambda| \geq 1$, we can form linear combinations $|q_1\bar{q}_2; \Lambda, \eta, \epsilon\,; \boldsymbol{r}\rangle$ analogous to Eq. (1) that are labelled by $\Lambda = |\lambda|$, η, and ϵ. These configurations are eigenstates of $R_{\rm light}$ with the eigenvalue ϵ.

The tetraquark potentials with flavor $q_1\bar{q}_2$ are energies of stationary configurations of light-quark and gluon fields. For $q_1, q_2 = u, d$, it is more convenient to use the isospin quantum numbers (I, I_3) to specify the flavor state: $(0, 0) = (u\bar{u} + d\bar{d})/\sqrt{2}$, $(1, +1) = -u\bar{d}$,

$(1,0) = (u\bar{u} - d\bar{d})/\sqrt{2}$, and $(1,-1) = d\bar{u}$. If we ignore small effects from the difference between the masses of the u and d quarks and their different electromagnetic charges, the energy of the configuration depends on the isospin quantum number I, which is 0 or 1, but not on I_3. Within the same approximation, the flavor configurations $u\bar{s}$ and $d\bar{s}$, which form an isospin doublet, and the flavor configurations $-s\bar{d}$ and $s\bar{u}$, which also form an isospin doublet, all have the same energies. Thus the only flavor labels required to specify the distinct energies of the tetraquark configurations are $I = 0$, $I = 1$, $s\bar{q}$, and $s\bar{s}$. The tetraquark potentials can be denoted $V_\Gamma^{(I=0)}(r)$, $V_\Gamma^{(I=1)}(r)$, $V_\Gamma^{(s\bar{q})}(r)$, and $V_\Gamma^{(s\bar{s})}(r)$, where $\Gamma = \Lambda_\eta^\epsilon$.

If we consider only flavor quantum numbers with no net strangeness (i.e. either $q_1\bar{q}_2$ with $q_1, q_2 = u, d$ or else $s\bar{s}$), the stationary light-field configurations with flavors $I = 0$, $I = 1$, and $s\bar{s}$ are also eigenstates of G-parity, which is the product of the charge conjugation operator C_{light} and an isospin rotation by angle π around the I_2 axis. Its eigenvalues are:

$$G = \eta\,\epsilon\,(-1)^{\Lambda+I}. \tag{2}$$

The neutral members of the isospin multiplets are eigenstates of C_{light} with eigenvalue $-G$.

C. Quarkonium potential

Conventional quarkonia are energy levels of a $Q\bar{Q}$ pair in the flavor-singlet Σ_g^+ potential. The limiting behaviors of the Σ_g^+ potential at large r and at small r are understood, at least in the absence of light quarks [23]. At large r, the field configuration for Σ_g^+ is a flux tube extending between the $\bar{Q}$ and Q. The potential approaches the ground-state energy of a relativistic string of length r with fixed endpoints [23]:

$$V_{\Sigma_g^+}(r) \longrightarrow \sigma r \left(1 - \frac{\pi}{6\sigma r^2}\right)^{1/2} + E_0, \tag{3}$$

where σ is the string tension, which is the energy per length of the flux tube, and E_0 is an additive constant. At small r, the Σ_g^+ potential approaches the attractive color-Coulomb potential between a Q and $\bar{Q}$ in a color-singlet state:

$$V_{\Sigma_g^+}(r) \longrightarrow -\frac{4\alpha_s(1/r)}{3r} + E_{\Sigma_g^+}, \tag{4}$$

where $\alpha_s(\mu)$ is the running coupling constant of QCD at the momentum scale μ and $E_{\Sigma_g^+}$ is an additive constant [23].

A simple phenomenological potential that is qualitatively compatible with the limiting behaviors in Eqs. (3) and (4) is the Cornell potential [24]:

$$V_{\Sigma_g^+}(r) = 2m_Q + V_0 - \frac{\kappa}{r} + \sigma r. \tag{5}$$

The parameter κ can be interpreted as an effective value of $(4/3)\alpha_s(1/r)$ in the small-r region. Alternatively, if the value of κ is close to $\pi/12 \approx 0.262$, it can be interpreted as a coefficient in the expansion of Eq. (3) at large r. The additive constant in Eq. (5) has been separated into $2m_Q$ and a term V_0 that is independent of the heavy quark. The parameters σ, κ, m_c, m_b and V_0 can all be determined phenomenologically by fitting the energy levels of conventional charmonium and bottomonium. Such a fit will be carried out in Section VI A.

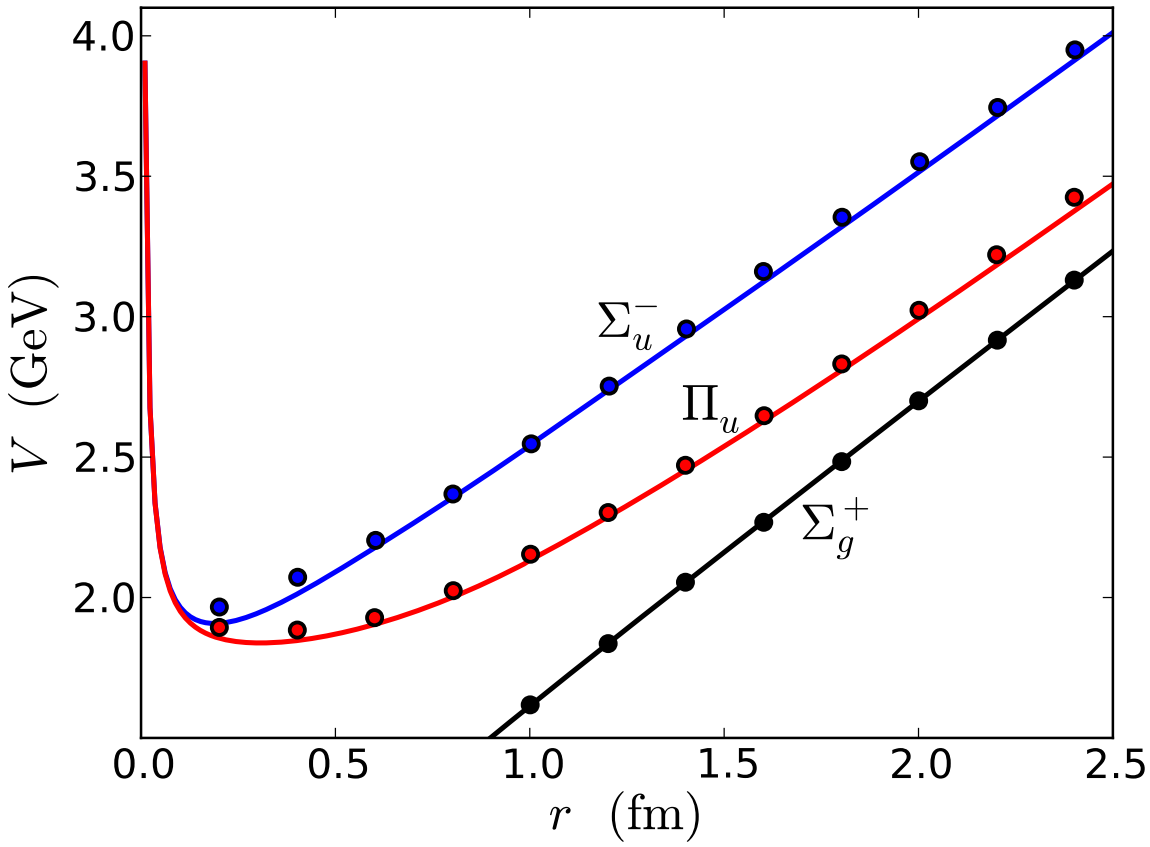

FIG. 1: The Σ_u^+, Π_u, and Σ_u^- Born-Oppenheimer potentials for conventional quarkonium and quarkonium hybrids. The dots are the potentials calculated using quenched lattice gauge theory in Ref. [13]. The curves are fits to those potentials.

The Σ_g^+ potential can be calculated using lattice QCD. The string tension σ defined by Eq. (3) can be used to set the length scale in lattice QCD calculations. However calculations of potentials in lattice QCD are more stable if the length scale is set instead by the Sommer radius r_0 [25] defined by

$$r_0^2 V'_{\Sigma_g^+}(r_0) = 1.65, \tag{6}$$

where $V'(r)$ represents the derivative of the potential with respect to r. A phenomenological value of this parameter obtained by fitting the bottomonium spectrum is $r_0^{-1} = 394 \pm 20$ MeV [26], so $r_0 \approx 0.50$ fm. A fit of the Σ_g^+ potential calculated using quenched lattice QCD to the Cornell potential gives $\kappa = 0.292(6)$ and $\sqrt{\sigma} r_0 = 1.165(3)$ [27], which implies $\sigma = 0.21 \pm 0.02$ GeV^2. The long-distance part of the potential calculated in Ref. [13] using quenched lattice gauge theory is shown in Fig. 1. If the potential is fit to Eq. (3), the string tension is determined to be $\sigma = 0.21$ GeV^2.

The Σ_g^+ potential has been calculated using lattice QCD with two flavors of dynamical light quarks [27]. A fit to the Cornell potential gives $\kappa = 0.368^{+20}_{-26}$ and $\sqrt{\sigma} r_0 = 1.133^{+11}_{-8}$, which implies $\sigma = 0.20 \pm 0.02$ GeV^2. The values of κ and $\sqrt{\sigma} r_0$ differ significantly from those calculated using quenched lattice QCD. The extrapolation of the Σ_g^+ potential crosses the threshold defined by twice the mass of the static meson near $r \approx 2.4\, r_0$. For $r > 2.4\, r_0$,

the minimal-energy prescription can not be used to define the Σ_g^+ potential. Lattice QCD has nevertheless been used to calculate the Σ_g^+ potential with high precision at larger values of r [28]. There is another B-O potential that approaches the threshold for a pair of static mesons as $r \to \infty$. It actually has an avoided crossing with the Σ_g^+ potential. Lattice QCD has been used to calculate the two potentials in the region of the avoided crossing [29].

D. Hybrid potentials

Quarkonium hybrid mesons are energy levels of a $Q\bar{Q}$ pair in the excited flavor-singlet B-O potentials. We will refer to these potentials as hybrid potentials. Many of the hybrid potentials were calculated by Juge, Kuti, and Morningstar using quenched lattice QCD [13, 23]. They all have minima at positive values of r. The deepest hybrid potentials are Π_u and Σ_u^-.

The limiting behaviors of the hybrid potentials at large r and at small r are understood, at least in the absence of light quarks [23]. At large r, the field configuration for the potential Γ is a flux tube extending between the Q and $\bar{Q}$. The corresponding potential approaches an excited energy level of a relativistic string of length r with fixed endpoints:

$$V_\Gamma(r) \longrightarrow \sigma r \left(1 + \frac{\pi(12n_\Gamma - 1)}{6\sigma r^2}\right)^{1/2} + E_0, \tag{7}$$

where the excitation number n_Γ depends on the B-O potential, and E_0 is the same additive constant as in Eq. (3). The Σ_g^+ potential, whose limiting behavior is given in Eq. (3), is the ground state of the string with $n_\Gamma = 0$. The Π_u potential is the first excited state with $n_\Gamma = 1$. The Σ_u^- potential has $n_\Gamma = 3$. The B-O potentials with $n_\Gamma = 2$ are Δ_g, Π_g, and the first excited Σ_g^+ potential, which is labelled $\Sigma_g^{+\prime}$. At small r, the hybrid potentials approach the repulsive color-Coulomb potential between a Q and $\bar{Q}$ in a color-octet state:

$$V_\Gamma(r) \longrightarrow +\frac{\alpha_s(1/r)}{6r} + E_\Gamma, \tag{8}$$

where E_Γ is an additive constant that depends on the B-O potential.

In the limit $r \to 0$, the Q and $\bar{Q}$ sources reduce to a single local color-octet $Q\bar{Q}$ source. In this limit, the conserved quantum numbers of the gluon and light-quark fields in the presence of the source are $J^{PC}_{\rm light}$. The energy levels of flavor-singlet gluon and light-quark field configurations bound to a static color-octet source are called *static hybrid mesons* or *gluelumps*. In QCD without light quarks, a gluelump can be defined as the minimal-energy configuration of the gluon field with specified quantum numbers $J^{PC}_{\rm light}$. In QCD with light quarks, the minimal-energy prescription can still be used to define the ground-state gluelump with quantum numbers 1^{+-}. The minimal-energy prescription can be used to define an excited gluelump only if its energy relative to the ground-state gluelump is less than $2m_\pi$ or $3m_\pi$, depending on the quantum numbers. Otherwise, the minimal-energy configuration is the ground-state 1^{+-} gluelump accompanied by 2 or 3 pions. In this case, the excited gluelump would have to be identified as one of the excited states of the gluon and light-quark fields with the appropriate $J^{PC}_{\rm light}$ quantum numbers in the presence of the static $Q\bar{Q}$ source.

In the limit $r \to 0$, the gluon and light-quark fields in the presence of the Q and $\bar{Q}$ sources have additional symmetries that require various B-O potentials to become degenerate in that

gluelumps		adjoint mesons		
J^{PC}	g	J^{PC}	$q\bar{q}$	$s\bar{s}$
1^{+-}	(0)	1^{--}	47 ± 90	120 ± 70
1^{--}	285 ± 53	0^{-+}	91 ± 216	170 ± 99
2^{--}	710 ± 37			

TABLE IV: Gluelump and adjoint meson energies (in MeV) relative to the energy of the 1^{+-} ground-state gluelump. The gluelump energies are from the lattice QCD calculations with dynamical light quarks in Ref. [33]. The adjoint meson energies are from the quenched lattice QCD calculations in Ref. [31]. The errors in the adjoint meson energies do not take into account systematic errors from omitting light-quark loops.

limit [30]. In the limiting expression in Eq. (8) for the hybrid potential at small r, the additive constant E_Γ can be interpreted as the energy of a gluelump. For the two deepest hybrid potentials, Π_u and Σ_u^-, E_Γ must be equal to the energy of the ground-state 1^{+-} gluelump. For the Π_g and $\Sigma_g^{+\prime}$ potentials, E_Γ must be equal to the energy of the 1^{--} gluelump. For the Δ_g potential, the Σ_g^- potential, and the first excited Π_g potential, which is labelled Π_g', E_Γ must be equal to the energy of the 2^{--} gluelump.

Given the quantum numbers $J^{PC}_{\rm light}$ of the gluelump, we can deduce the hybrid potentials whose additive constant E_Γ defined by Eq. (8) is equal to the energy of the gluelump. A component of the angular momentum vector for a gluelump with spin $J_{\rm light}$ has $2J_{\rm light}+1$ integer values ranging from $-J_{\rm light}$ to $+J_{\rm light}$. There must therefore be a B-O potential for each integer value of Λ from 0 up to $J_{\rm light}$. The quantum number η for all these potentials equals the value of $(CP)_{\rm light}$ for the gluelump. One of the B-O potentials must be a Σ potential with $\Lambda = 0$. If we identify its reflection quantum number as $\epsilon = P_{\rm light}(-1)^{J_{\rm light}}$, the Σ potentials associated with the 1^{+-}, 1^{--}, and 2^{--} gluelumps are correctly inferred to be Σ_u^-, $\Sigma_g^{+\prime}$, and Σ_g^-, respectively.

The gluelump spectrum was first calculated using quenched lattice QCD by Campbell, Jorysz, and Michael [31]. The ground-state gluelump was found to have quantum numbers 1^{+-}. More accurate results for the gluelump energy differences were calculated subsequently by Foster and Michael [32]. The gluelump spectrum was recently calculated by Marsh and Lewis using lattice QCD with dynamical light quarks [33]. The strange quark had its physical mass, but the up and down quark masses were unphysically heavy, corresponding to a pion mass of about 500 MeV. The first two excited states of the gluelump have quantum numbers 1^{--} and 2^{--}. Their energies relative to that of the ground-state 1^{+-} gluelump are given in Table IV. The energies of the 1^{--} and 2^{--} gluelumps are higher by about 300 MeV and 700 MeV, respectively.

The hybrid potentials can be calculated using lattice QCD. In Ref. [13], quenched lattice QCD was used to calculate many of these potentials. They interpolate between the short-distance limit in Eq. (8) and the long-distance limit in Eq. (7). The Π_u and Σ_u^- potentials from Ref. [13] are shown in Fig. 1.

An accurate parametrization of the Π_u potential in Ref. [13] at short and intermediate distances was given in Ref. [34]:

$$V_{\Pi_u}(r) = E_{\Pi_u} + 0.11\frac{1}{r} + 0.24\frac{r^2}{r_0^3}, \tag{9}$$

where $r_0 \approx 0.50$ fm is the Sommer radius defined in Eq. (6). This parametrization provides an excellent fit to the Π_u potential at lattice spacings between $0.3\,r_0$ and $2.4\,r_0$. The minimum of the potential is at $0.61 r_0 \approx 0.3$ fm. The Π_u potential has also been calculated for QCD with two flavors of dynamical light quarks [27]. No statistically significant differences were found between the Π_u potentials with and without light quarks.

An important feature of the parametrization of the Π_u potential in Eq. (9) is the absence of a linear term in r. The $1/r$ term can be interpreted as the repulsive color-Coulomb potential between the Q and $\bar{Q}$. The remaining terms can be interpreted as the energy of the gluon field configuration. According to the parametrization in Eq. (9), the gluon field energy has zero slope at $r = 0$, so it increases slowly with r in the small-r region. At $r = 0$, the gluon field configuration is the ground-state gluelump. At $r = r_0$, the gluon field energy has increased by less than 1/3 of the energy difference for the first excited gluelump. The slow increase of the gluon field energy with r is consistent with the gluon field configuration remaining close to the gluelump out to values of r comparable to r_0. At these small values of r, the configuration is compatible with the simple constituent model of a quarkonium hybrid meson: $(Q\bar{Q})_8 + g$. The constituent gluon g can be identified with the ground-state gluelump with quantum numbers 1^{+-}.

We can obtain a global fit to the potential $V_{\Pi_u}(r)$ by using the parametrization in Eq. (9) for r below some matching radius r_* and then switching to the string potential in Eq. (7) with $n_\Gamma = 1$ for r beyond r_*. We demand continuity of the potentials and their slopes at the matching point r_*:

$$E_{\Pi_u} - E_0 + 0.11\frac{1}{r_*} + 0.24\frac{r_*^2}{r_0^3} = \sigma\sqrt{r_*^2 + 11\pi/(6\sigma)}, \tag{10a}$$

$$-0.11\frac{1}{r_*} + 0.48\frac{r_*^2}{r_0^3} = \frac{\sigma r_*^2}{\sqrt{r_*^2 + 11\pi/(6\sigma)}}. \tag{10b}$$

These two equattions determine r_* and $E_{\Pi_u} - E_0$. If we take the value $\sqrt{\sigma} = 0.21\ r_0^{-1}$ from the fit to the long-distance part of the Σ_g^+ potential in Ref. [23], which is shown in Fig. 1, the matching point is determined by Eq. (10b) to be $r_* = 2.0\,r_0$. The difference between the energy offsets is then determined by Eq. (10a) to be $E_{\Pi_u} - E_0 = 2.8\,r_0^{-1}$. In Fig. 1, the resulting parametrization of $V_{\Pi_u}(r)$ is compared to the potential calculated using quenched lattice QCD in Ref. [23]. It gives a good fit over the entire range of r. The fit could be slightly improved by relaxing the constraint that the long-distance limits of the ground-state Σ_g^+ potential in Eq. (3) and the excited-state potentials Γ in Eq. (7) have the same additive constant E_0.

To obtain a parametrization of the Σ_u^- potential, it is most convenient to fit the difference between the Σ_u^- and Π_u potentials. In the quenched lattice QCD calculations in Ref. [23], that difference appears to be linear in r at small r. In Ref. [35], the splitting between $V_{\Sigma_u^-}(r)$ and $V_{\Pi_u}(r)$ was calculated in the region $r < 1.6\ r_0$ using quenched lattice QCD with a finer lattice. The results are consistent with those of Ref. [23], but they extend down to smaller values of r. For $r < 0.8\ r_0$, the splitting is compatible with quadratic dependence on r, and it can be fit with $0.92\ r^2/r_0^3$. Given the constraint provided by this leading power of r^2, the difference between the potentials in Ref. [23] can be fit very well with the simple parametrization

$$V_{\Sigma_u^-}(r) = V_{\Pi_u}(r) + \frac{0.92\ r^2/r_0^3}{1 + 0.63\ r^2/r_0^2}. \tag{11}$$

The minimum of the Σ_u^- potential is near $0.4\ r_0 \approx 0.2$ fm. In Fig. 1, the parametrization of $V_{\Sigma_u^-}(r)$ is compared to the potential calculated using quenched lattice QCD in Ref. [23]. It gives a good fit over the entire range of r. It will not give a good fit for $r > 2.5$ fm, because the parametrization in Eq. (11) does not take into account the constraints from the large-r limit given by Eq. (7).

E. Tetraquark potentials

Quarkonium tetraquark mesons are energy levels in B-O potentials with nonsinglet flavor quantum numbers, such as $q_1\bar{q}_2$. We will refer to these potentials as tetraquark potentials. The distinct B-O potentials can be specified by the flavor labels $I = 0$, $I = 1$, $s\bar{q}$, and $s\bar{s}$ and by the quantum numbers $\Gamma = \Sigma_\eta^+, \Sigma_\eta^-, \Pi_\eta, \Delta_\eta, \ldots$ for the light-quark and gluon field configuration. None of the tetraquark potentials have yet been calculated using lattice QCD.

The only information about the tetraquark potentials that is known from lattice QCD comes from calculations of *static adjoint mesons*, which are energy levels of light-quark and gluon fields with nonsinglet flavor quantum numbers bound to a static color-octet source. The conserved quantum numbers for the light fields in the presence of the source are $J^P_{\rm light}$ and the flavor quantum numbers. The charge conjugation operator $C_{\rm light}$ that changes a $q_1\bar{q}_2$ configuration into a $q_2\bar{q}_1$ configuration is also a symmetry operator. Foster and Michael have calculated the adjoint meson spectrum using quenched lattice QCD with a light valence quark and antiquark [32]. The adjoint meson energies were calculated for two values of the common mass of the light valence quark q and antiquark $\bar{q}$, one comparable to the physical mass of the s quark and one larger. This allowed for an extrapolation to the very small mass of the u and d quarks. The adjoint mesons with the lowest energies were found to be a vector with $J^{PC}_{\rm light} = 1^{--}$ and a pseudoscalar with $J^{PC}_{\rm light} = 0^{-+}$. Their energies relative to that of the ground-state 1^{+-} gluelump are given in Table IV. For $s\bar{s}$ adjoint mesons, the difference between the energies of the pseudoscalar and vector was 50 ± 70 MeV, so the vector is favored to be lower in energy. The extrapolation of this energy difference to light $q\bar{q}$ had larger error bars. The energy of the $s\bar{s}$ vector adjoint meson is larger than that of the $q\bar{q}$ vector adjoint meson by 73 ± 55 MeV. The difference between the energies of the $q\bar{q}$ vector adjoint meson and the ground-state 1^{+-} gluelump was 50 ± 90 MeV, favoring the gluelump to be lower in energy. The statistical errors in the energies of the ground-state gluelump, the light vector adjoint meson, and the light pseudoscalar adjoint meson are larger than the energy differences, so the ordering of their energies in quenched lattice QCD has not yet been established.

In QCD with two flavors of very light quarks u and d, the lightest adjoint mesons form an isospin triplet with $I = 1$ and an isospin singlet with $I = 0$. For the isospin singlet and the neutral member of the isospin triplet, the $J^{PC}_{\rm light}$ quantum number are 1^{--} for the vector and 0^{-+} for the pseudoscalar. The appropriate quantum numbers for the charged adjoint mesons are $I^G(J^P_{\rm light})$, where $G = (-1)^I C_{\rm light}$ and $C_{\rm light}$ is the charge conjugation quantum number of the neutral member of the multiplet. The vector adjoint mesons have quantum numbers $0^-(1^-)$ and $1^+(1^-)$. The pseudoscalar adjoint mesons have quantum numbers $0^+(0^-)$ and $1^-(0^-)$. Calculations of the adjoint meson spectrum using lattice QCD with dynamical light quarks are required to determine the ordering in energy of the ground-state gluelump and the four lowest-energy adjoint mesons with quantum numbers are $0^-(1^-)$, $1^+(1^-)$, $0^+(0^-)$, and $1^-(0^-)$. The energies of these adjoint mesons can be determined by a simple minimal-energy prescription if they do not exceed the energy of the ground-state gluelump by more

than $2m_\pi$, m_π, $2m_\pi$, and $3m_\pi$, respectively.

The existence of a static adjoint meson bound to a local color-octet source guarantees the existence of corresponding tetraquark potentials in the small-r region. Their behavior in this region is that of the repulsive color-Coulomb potential for a color-octet $Q\bar{Q}$ pair, analogous to Eq. (8). The additive constant analogous to E_Γ can be interpreted as the energy of the adjoint meson. Given the quantum numbers $J^P_{\rm light}$ of an adjoint meson, we can deduce the B-O potentials for which the additive constant E_Γ defined by Eq. (8) is equal to the energy of the adjoint meson. A component of the angular momentum vector for an adjoint meson with spin $J_{\rm light}$ has $2J_{\rm light}+1$ integer values ranging from $-J_{\rm light}$ to $+J_{\rm light}$. There must therefore be a B-O potential for each integer value of Λ from 0 up to $J_{\rm light}$. The quantum number η for the B-O potentials is the value of $(CP)_{\rm light}$ for a $q\bar{q}$ adjoint meson. One of the B-O potentials is a Σ potential with $\Lambda = 0$. Its reflection quantum number is $\epsilon = (-1)^{J_{\rm light}} P_{\rm light}$. The B-O potentials whose additive constant as $r \to 0$ equals the energy of the vector adjoint meson with $J^P_{\rm light} = 1^-$ are Π_g and Σ_g^+. The B-O potential whose additive constant is equal to the energy of the pseudoscalar adjoint meson with $J^P_{\rm light} = 0^-$ is Σ_u^-.

The behavior of the tetraquark potentials as r increases is not known. If a $q_1\bar{q}_2$ B-O potential can be defined at large r, the light-field configuration could be a flux tube extending between the Q and $\bar{Q}$ sources to which an excitation with the flavor quantum numbers $q_1\bar{q}_2$ is bound. In this case, the B-O potential would increase linearly at large r. One possibility is that the flavor q_1 is localized near the Q source to form a diquark with color charge $\bar{3}$, and that the flavor $\bar{q}_2$ is localized near the $\bar{Q}$ source to form an antidiquark with color charge 3. In this case, the flux tube between the diquark and the antidiquark would be essentially the same as a flavor-singlet flux tube between $\bar{Q}$ and Q sources. At large r, the B-O potential should approach the energy of a relativistic string as in Eq. (7) for some appropriate excitation number n_Γ and with a different energy offset to account for the energy difference between the Qq diquark and a Q source. We will assume that tetraquark potentials can be defined for all r, and that they have the same qualitative behavior as the hybrid potentials, with a minimum at a positive value of r.

We can use the information from quenched lattice QCD calculations on the lowest-energy adjoint mesons to infer which tetraquark potentials are likely to be the deepest. The hybrid potentials that are the lowest at small r are also the deepest hybrid potentials. We will assume that the tetraquark potentials have the same behavior. The tetraquark potentials that are the lowest at small r are Π_g, Σ_g^+, and Σ_u^-. They are therefore also likely to be the deepest tetraquark potentials. There should be Π_g, Σ_g^+, and Σ_u^- potentials for each of the flavor labels $I = 0$, $I = 1$, $s\bar{q}$, and $s\bar{s}$. We will assume that these tetraquark potentials have the same qualitative behavior as the hybrid potentials, with a minimum at a positive value of r.

In Ref. [11], simple assumptions on the behavior of the isospin-1 B-O potentials were used to estimate masses for quarkonium tetraquarks. The deepest isospin-1 B-O potentials were assumed to be the same as for the flavor-singlet case, namely Π_u and Σ_u^-. This assumption was simply a guess, with no motivation from QCD. The Σ_u^- potential coincides with one of the three deepest tetraquark potentials inferred from the lowest energy adjoint mesons.

IV. BORN-OPPENHEIMER ENERGY LEVELS

In this section, we discuss the energy levels of a $Q\bar{Q}$ pair in the Born-Oppenheimer (B-O) potentials, which can be identified with $Q\bar{Q}$ mesons. We deduce the quantum numbers of the $Q\bar{Q}$ mesons and we also derive selection rules for hadronic transitions between them.

A. Angular momenta

When we take into account the motion and spin of the heavy quark and antiquark, there are several angular momenta that contribute to the spin vector $\boldsymbol{J}$ of the meson. In addition to the total angular momentum $\boldsymbol{J}_{\rm light}$ of the gluon and light-quark fields, there is the orbital angular momentum $\boldsymbol{L}_{Q\bar{Q}}$ of the $Q\bar{Q}$ pair and the spins of the Q and $\bar{Q}$. We denote the total spin of the $Q\bar{Q}$ pair by $\boldsymbol{S}$. It is convenient to introduce an angular momentum $\boldsymbol{L}$ that is the sum of all the angular momenta excluding the spins of the heavy quark and antiquark. The spin vector of the meson can then be expressed as

$$\boldsymbol{J} = \boldsymbol{L} + \boldsymbol{S}, \tag{12a}$$

$$\boldsymbol{L} = \boldsymbol{L}_{Q\bar{Q}} + \boldsymbol{J}_{\rm light}. \tag{12b}$$

The condition that $\boldsymbol{L}_{Q\bar{Q}}$ is orthogonal to the separation vector $\boldsymbol{r}$ of the Q and $\bar{Q}$ can be expressed as

$$\hat{\boldsymbol{r}} \cdot \boldsymbol{L} = \hat{\boldsymbol{r}} \cdot \boldsymbol{J}_{\rm light} = \lambda, \tag{13}$$

where λ is the quantum number introduced in Section III B. The constraint in Eq. (13) puts a lower limit on the quantum number L for $\boldsymbol{L}^2$: $L \geq \Lambda$, where $\Lambda = |\lambda|$.

The centrifugal energy of the $Q\bar{Q}$ pair is proportional to the square of their orbital angular momentum:

$$\boldsymbol{L}_{Q\bar{Q}}^2 = \boldsymbol{L}^2 - 2\boldsymbol{L} \cdot \boldsymbol{J}_{\rm light} + \boldsymbol{J}_{\rm light}^2. \tag{14}$$

Imposing the constraint in Eq. (13), this can be expressed as

$$\boldsymbol{L}_{Q\bar{Q}}^2 = \boldsymbol{L}^2 - 2\Lambda^2 + \boldsymbol{J}_{\rm light}^2 - \left(L_+ J_{\rm light,-} + L_- J_{\rm light,+}\right), \tag{15}$$

where L_+ and L_- are raising and lowering operators for $\hat{\boldsymbol{r}} \cdot \boldsymbol{L}$ and $J_{\rm light,+}$ and $J_{\rm light,-}$ are raising and lowering operators for $\hat{\boldsymbol{r}} \cdot \boldsymbol{J}_{\rm light}$.

B. Schroedinger equation

The B-O approximation consists of two distinct approximations. The first approximation is an *adiabatic approximation*, in which the instantaneous configuration of the gluon and light-quark fields is assumed to be a stationary state in the presence of static sources at the positions of the Q and $\bar{Q}$. The stationary states can be labelled by the quantum numbers $\Gamma = \Lambda_\eta^\epsilon$ introduced in Section III B and by light-quark flavor quantum numbers. This approximation reduces the problem to a multi-channel nonrelativistic Schroedinger equation for the Q and $\bar{Q}$. The multi-component wavefunction has a component for every B-O configuration Γ allowed by the symmetries of QCD. The discrete solutions to the multichannel Schroedinger equation correspond to $Q\bar{Q}$ mesons with definite J^P quantum numbers. This adiabatic approximation ignores effects that are suppressed by powers of $\Lambda_{\rm QCD}/m_Q$

and by powers of v^2, where v is the typical relative velocity of the $Q\bar{Q}$ pair, so it becomes increasingly accurate as the heavy quark mass increases. The second approximation is a *single-channel approximation* in which all components of the wavefunction are ignored except that for a single B-O configuration Γ. This approximation breaks down in regions of r where the B-O potential for Γ has avoided crossings with other B-O potentials. It can only be a good approximation if the wavefunction is sufficiently small in those regions.

With the combination of the adiabatic approximation and the single-channel approximation, the Schroedinger equation for the $Q\bar{Q}$ pair in the presence of a stationary configuration Γ of the gluon and light-quark fields can be expressed as

$$\left[-\frac{1}{m_Q}\langle \boldsymbol{D}^2\rangle_{\Gamma,\boldsymbol{r}} + V_\Gamma(r)\right]\psi(\boldsymbol{r}) = E\psi(\boldsymbol{r}), \tag{16}$$

where the subscript $\Gamma, \boldsymbol{r}$ on the expectation value implies that it is evaluated in the configuration Γ for Q and $\bar{Q}$ sources that are separated by $\boldsymbol{r}$. The covariant derivative $\boldsymbol{D}$ has a term with a gluon field that is responsible for retardation effects. Since retardation effects are suppressed by powers of v, ignoring these terms is consistent with the adiabatic approximation. The covariant Laplacian $\boldsymbol{D}^2$ can therefore be replaced by an ordinary Laplacian, which includes a centrifugal term proportional to $\boldsymbol{L}^2_{Q\bar{Q}}$:

$$\left[-\frac{1}{m_Q}\left(\frac{d}{dr}\right)^2 + \frac{\langle \boldsymbol{L}^2_{Q\bar{Q}}\rangle_{\Gamma,\boldsymbol{r}}}{m_Q r^2} + V_\Gamma(r)\right] r\psi(\boldsymbol{r}) = Er\psi(\boldsymbol{r}). \tag{17}$$

In the expression for $\boldsymbol{L}^2_{Q\bar{Q}}$ in Eq. (15), the last term is a linear combination of $J_{\mathrm{light},+}$ and $J_{\mathrm{light},-}$. In the multi-channel Schroedinger equation, these terms provide couplings to other components of the wavefunction with Λ larger by 1 or smaller by 1. The single-channel approximation eliminates any contribution from these terms. If the wavefunction is an eigenstate of $\boldsymbol{L}^2$ with angular momentum quantum number L, the expectation value of $\boldsymbol{L}^2_{Q\bar{Q}}$ can be expressed as

$$\langle \boldsymbol{L}^2_{Q\bar{Q}}\rangle_{\Gamma,\boldsymbol{r}} = L(L+1) - 2\Lambda^2 + \langle \boldsymbol{J}^2_{\mathrm{light}}\rangle_{\Gamma,\boldsymbol{r}}. \tag{18}$$

Since $\boldsymbol{J}^2_{\mathrm{light}}$ is a scalar operator, the function $\langle \boldsymbol{J}^2_{\mathrm{light}}\rangle_{\Gamma,\boldsymbol{r}}$ depends on r only. A wavefunction $\psi(\boldsymbol{r})$ that is a simultaneous eigenstate of $\boldsymbol{L}^2$ and L_z with angular momentum quantum numbers L and m_L can be expressed in the form $R(r)Y_{Lm_L}(\hat{\boldsymbol{r}})$, where $R(r)$ is a radial wavefunction and $Y_{Lm_L}(\hat{\boldsymbol{r}})$ is a spherical harmonic. The Schroedinger equation in Eq. (17) then reduces to the radial Schroedinger equation

$$\left[-\frac{1}{m_Q}\left(\frac{d}{dr}\right)^2 + \frac{L(L+1) - 2\Lambda^2 + \langle \boldsymbol{J}^2_{\mathrm{light}}\rangle_{\Gamma,\boldsymbol{r}}}{m_Q r^2} + V_\Gamma(r)\right] rR(r) = ErR(r). \tag{19}$$

In the pioneering work on the B-O approximation for quarkonium hybrids in Ref. [13], the authors assumed without much justification that $\langle \boldsymbol{J}^2_{\mathrm{light}}\rangle_{\Gamma,\boldsymbol{r}}$ was 0 for the quarkonium potential Σ_g^+ and 2 for the quarkonium hybrid potentials Π_u and Σ_u^-. There is a lower bound on the expectation value in a state with $\hat{\boldsymbol{r}}\cdot\boldsymbol{J}_{\mathrm{light}} = \lambda$: $\langle \boldsymbol{J}^2_{\mathrm{light}}\rangle \geq \Lambda(\Lambda+1)$. The authors assumed that this lower bound is saturated in the case of Σ_g^+, for which $\Lambda = 0$, and in the case of Π_u, for which $\Lambda = 1$. Their assumption that $\langle \boldsymbol{J}^2_{\mathrm{light}}\rangle_{\Gamma,\boldsymbol{r}} = 2$ for Π_u and Σ_u^- is consistent with a constituent-gluon model in which the $Q\bar{Q}$ pair is accompanied by a spin-1 constituent gluon with $\boldsymbol{J}^2_{\mathrm{light}} = 2$.

There is a more compelling motivation for setting $\langle \boldsymbol{J}^2_{\rm light}\rangle_{\Gamma,\boldsymbol{r}} = 2$ for Π_u and Σ_u^-. The centrifugal term in the energy is most important at small $\boldsymbol{r}$, where it provides a centrifugal barrier. At $\boldsymbol{r} = 0$, the light-field configurations for both Π_u and Σ_u^- reduce to the ground-state gluelump with quantum numbers 1^{+-}. The gluelump is an eigenstate of $\boldsymbol{J}^2_{\rm light}$ with eigenvalue 2. Thus the function $\langle \boldsymbol{J}^2_{\rm light}\rangle_{\Gamma,\boldsymbol{r}}$ must be equal to 2 at $\boldsymbol{r} = 0$. In order for $\langle \boldsymbol{J}^2_{\rm light}\rangle_{\Gamma,\boldsymbol{r}} \approx 2$ to give a good approximation to the solution of the Schroedinger equation, it is not necessary for it to be a good approximation to the function at all $\boldsymbol{r}$. It only needs to be a good approximation in the region of small $\boldsymbol{r}$ where the centrifugal term is important. It should be a good approximation in that region if the light-field configuration only departs slowly from that of the gluelump as r increases. The same reasoning applied to a potential $V_\Gamma(r)$ whose additive constant as $r \to 0$ is the energy of a gluelump with spin J_Γ implies that the appropriate approximation is

$$\langle \boldsymbol{J}^2_{\rm light}\rangle_{\Gamma,\boldsymbol{r}} \approx J_\Gamma(J_\Gamma + 1). \tag{20}$$

For the Π_g and $\Sigma_g^{+\prime}$ potentials, whose additive constant as $r \to 0$ is the energy of the 1^{--} gluelump, the appropriate approximation is $\langle \boldsymbol{J}^2_{\rm light}\rangle \approx 2$. For the Δ_g, Π_g', and $\Sigma_g^{-\prime}$ potentials, whose additive constant as $r \to 0$ is the energy of the 2^{--} gluelump, the appropriate approximation is $\langle \boldsymbol{J}^2_{\rm light}\rangle \approx 6$. Similar logic can be applied to the Schroedinger equation for $Q\bar{Q}$ mesons with light-quark flavors. In this case, J_Γ would be the spin of the static adjoint meson whose energy determines the additive constant in the tetraquark potential as $r \to 0$.

The approximation in Eq. (20) should be a good one if the light-field configuration departs slowly from the gluelump as r increases. Accurate parametrizations of the Π_u and Σ_u^- potentials are given in Eqs. (9) and (11). The absence of linear terms in r implies that the energies of the Π_u and Σ_u^- configurations remain close to the energy of the ground-state gluelump until r becomes comparable to r_0. This is consistent with the assumption that the Π_u and Σ_u^- configurations themselves remain close to the gluelump until r becomes comparable to r_0. This suggests that the approximation in Eq. (20) is probably very good in the short-distance region where the centrifugal term in the potential is most important.

When the approximation for $\langle \boldsymbol{J}^2_{\rm light}\rangle_{\Gamma,\boldsymbol{r}}$ in Eq. (20) is inserted into the radial Schroedinger equation in Eq. (19), the function in the numerator of the centrifugal term becomes a number:

$$\left[-\frac{1}{m_Q}\left(\frac{d}{dr}\right)^2 + \frac{L(L+1) - 2\Lambda^2 + J_\Gamma(J_\Gamma+1)}{m_Q r^2} + V_\Gamma(r)\right] rR(r) = ErR(r). \tag{21}$$

The possible values of the orbital-angular-momentum quantum number L are $\Lambda, \Lambda+1, \ldots$. The radial excitations can be labelled by a principal quantum number $n = 1, 2, 3, \ldots$.

C. Meson quantum numbers

For each B-O configuration Γ, the solution to the radial Schroedinger equation in Eq. (21) gives energy levels E_{nL} and wavefunctions $R_{nL}(r)Y_{Lm_L}(\hat{\boldsymbol{r}})$. The hybrid configurations are labelled by $\Gamma = \Lambda_\eta^\epsilon$. The energy levels correspond to configurations of the Q and $\bar{Q}$ and the light fields of the form

$$\big|nLm_L Sm_S; \Lambda, \eta, \epsilon\big\rangle = \int d^3r\, R_{nL}(r)Y_{Lm_L}(\hat{\boldsymbol{r}})\big|\Lambda, \eta, \epsilon\,; \boldsymbol{r}\big\rangle\big|Sm_S\big\rangle, \tag{22}$$

quarkonia and hybrids			$q\bar{q}$ tetraquarks		
$\Gamma(nL)$	$S=0$	$S=1$	$\Gamma(nL)$	$S=0$	$S=1$
$\Sigma_g^+(1S)$	0^{-+}	1^{--}	$\Pi_g^-(1P)$	1^{+-}	$(0,1,2)^{++}$
$\Sigma_g^+(1P)$	1^{+-}	$(0,1,2)^{++}$	$\Pi_g^-(1D)$	2^{-+}	$(1,2,3)^{--}$
$\Sigma_g^+(1D)$	2^{-+}	$(1,2,3)^{--}$	$\Pi_g^-(1F)$	3^{+-}	$(2,3,4)^{++}$
$\Pi_u^+(1P)$	1^{--}	$(0,\mathbf{1},2)^{-+}$	$\Pi_g^+(1P)$	$\mathbf{1}^{-+}$	$(\mathbf{0},1,2)^{--}$
$\Pi_u^+(1D)$	2^{++}	$(1,\mathbf{2},3)^{+-}$	$\Pi_g^+(1D)$	$\mathbf{2}^{+-}$	$(1,2,3)^{++}$
$\Pi_u^+(1F)$	3^{--}	$(2,\mathbf{3},4)^{-+}$	$\Pi_g^+(1F)$	$\mathbf{3}^{-+}$	$(2,3,4)^{--}$
$\Pi_u^-(1P)$	1^{++}	$(\mathbf{0},1,\mathbf{2})^{+-}$	$\Sigma_g^+(1S)$	0^{-+}	1^{--}
$\Pi_u^-(1D)$	2^{--}	$(\mathbf{1},2,\mathbf{3})^{-+}$	$\Sigma_g^+(1P)$	1^{+-}	$(0,1,2)^{++}$
$\Pi_u^-(1F)$	3^{++}	$(\mathbf{2},3,\mathbf{4})^{+-}$	$\Sigma_g^+(1D)$	2^{-+}	$(1,2,3)^{--}$
$\Sigma_u^-(1S)$	0^{++}	1^{+-}	$\Sigma_u^-(1S)$	0^{++}	1^{+-}
$\Sigma_u^-(1P)$	1^{--}	$(0,\mathbf{1},2)^{-+}$	$\Sigma_u^-(1P)$	1^{--}	$(0,\mathbf{1},2)^{-+}$
$\Sigma_u^-(1D)$	2^{++}	$(1,\mathbf{2},3)^{+-}$	$\Sigma_u^-(1D)$	2^{++}	$(1,\mathbf{2},3)^{+-}$

TABLE V: Spin-symmetry multiplets for the ground state and the first two orbital-angular-momentum excitations in the quarkonium potential Σ_g^+, the two deepest hybrid potentials Π_u and Σ_u^-, and the Π_g, Σ_g^+, and Σ_u^- potentials for $q\bar{q}$ tetraquarks. A bold $\boldsymbol{J}$ indicates that $\boldsymbol{J}^{PC}$ is an exotic quantum number that is not possible if the constituents are only $Q\bar{Q}$.

where $|\Lambda,\eta,\epsilon\,;\boldsymbol{r}\rangle$ is the light-field configuration defined in Eq. (1) and $|Sm_S\rangle$ is the spin state of the $Q\bar{Q}$ pair, which can be singlet ($S=0$) or triplet ($S=1$). The state in Eq. (22) is an eigenstate of P and C:

$$P \;=\; \epsilon\,(-1)^{\Lambda+L+1}, \tag{23a}$$

$$C \;=\; \eta\,\epsilon\,(-1)^{\Lambda+L+S}. \tag{23b}$$

The eigenvalue of CP is the product of η for the light-field configuration and $(-1)^{S+1}$ for the spin state of the $Q\bar{Q}$ pair. The eigenvalue of the parity operator P is the product of $\epsilon(-1)^{\Lambda}$ for the light-field configuration, $(-1)^L$ for the spherical harmonic, and -1 for the opposite intrinsic parities of the Q and $\bar{Q}$.

Mesons are states with definite quantum numbers for the angular momentum $\boldsymbol{J}=\boldsymbol{L}+\boldsymbol{S}$. For flavor-singlet $Q\bar{Q}$ mesons, the configurations of the Q and $\bar{Q}$ and light fields with definite angular-momentum quantum numbers J and m_J are linear combinations of those in Eq. (22) with Clebsch-Gordan coefficients:

$$\big|nLSJm_J;\Lambda,\eta,\epsilon\big\rangle = \sum_{m_L m_S} \langle Lm_L,Sm_S|Jm_J\rangle \big|nLm_L Sm_S;\Lambda,\eta,\epsilon\big\rangle. \tag{24}$$

In the spin-singlet case ($S=0$), J equals L. In the spin-triplet case ($S=0$), J ranges from $|L-1|$ to $L+1$ in integer steps. The parity and charge conjugation quantum numbers P and C for the meson are given in Eqs. (23).

The $Q\bar{Q}$ mesons are conveniently organized into spin-symmetry multiplets consisting of states with the same B-O configuration $\Gamma=\Lambda_\eta^\epsilon$, radial quantum number n, orbital-angular-momentum quantum number L, and flavor. The states in these multiplets are related by heavy-quark spin symmetry. Ordinary quarkonia are energy levels in the flavor-singlet Σ_g^+

potential. We set $\Lambda = 0$ and $J_\Gamma = 0$ in the Schroedinger equation in Eq. (21). The possible values of L are $0, 1, 2, \ldots$ (or equivalently $S, P, D, \ldots$). The spin-symmetry multiplets for the ground state $1S$ and the first two orbital-angular-momentum excitations $1P$ and $1D$ are given in Table V.

The lowest-energy quarkonium hybrids are energy levels in the flavor-singlet Π_u and Σ_u^- potentials, whose short-distance behaviors are determined by the 1^{+-} gluelump. For the deepest hybrid potential Π_u, we set $\Lambda = 1$ and $J_\Gamma = 1$ in the Schroedinger equation in Eq. (21). The possible values of L are $1, 2, 3, \ldots$ (or equivalently $P, D, F, \ldots$). The spin-symmetry multiplets for the ground state $1P$ and the first two orbital-angular-momentum excitations $1D$ and $1F$ are given in Table V for both the Π_u^+ and Π_u^- configurations. For the next deepest hybrid potential Σ_u^-, we set $\Lambda = 0$ and $J_\Gamma = 1$ in the Schroedinger equation in Eq. (21). The spin-symmetry multiplets for the ground state $1S$ and the first two orbital-angular-momentum excitations $1P$ and $1D$ are given in Table V.

Tetraquark $Q\bar{Q}$ mesons are energy levels in potentials labelled by quantum numbers $\Gamma = \Lambda_\eta^\epsilon$ for the B-O configuration and by flavor quantum numbers. The flavor labels for distinct B-O potentials are $I = 1$, $I = 0$, $s\bar{q}$, and $s\bar{s}$. The lowest-energy quarkonium tetraquarks are expected to be energy levels in the Π_g, Σ_g^+, and Σ_u^- potentials. Their multiplets are most easily specified by giving the J^{PC} quantum numbers of $q\bar{q}$ tetraquark mesons. For the Π_g and Σ_g^+ potentials, Λ is 1 and 0, respectively, and $J_\Gamma = 1$, because the short-distance behavior is determined by the 1^{--} adjoint meson. For the Σ_u^- potential, $\Lambda = 0$ and $J_\Gamma = 0$, because the short-distance behavior is determined by the 0^{-+} adjoint meson. The spin-symmetry multiplets for the ground state and the first two orbital-angular-momentum excitations of the Π_g^-, Π_g^+, Σ_g^+, and Σ_u^- configurations are given in Table V.

The J^{PC} quantum numbers for $q\bar{q}$ tetraquarks in Table V apply to the $I = 0$ tetraquark, the $s\bar{s}$ tetraquark, and the neutral member of the $I = 1$ isospin triplet. The isospin triplet has spin-symmetry multiplets whose states have G-parity $G = -C$ and the J^P quantum numbers of the $q\bar{q}$ tetraquarks in Table V. The strange tetraquark mesons containing $u\bar{s}$ or $d\bar{s}$ form isospin doublets whose spin-symmetry multiplets have the J^P quantum numbers of the $q\bar{q}$ tetraquarks in Table V.

D. Selection rules

Many of the decay modes of the XYZ mesons listed in Tables I, II, and III are hadronic transitions to another $Q\bar{Q}$ meson. Selection rules for the hadronic transitions provide essential constraints on the quarkonium hybrids or quarkonium tetraquarks that can be considered as candidates for specific XYZ mesons. The selection rules govern changes in the angular momentum quantum numbers L, S, and J of the $Q\bar{Q}$ meson and changes in the quantum numbers Λ, η, and ϵ that specify the light-field configuration. For simplicity, we will deduce the selection rules for transitions between neutral $Q\bar{Q}$ mesons with definite J^{PC} quantum numbers. The corresponding selection rules involving charged tetraquark mesons that belong to an isospin triplet with quantum numbers $1^G(J^P)$ can be inferred from the selection rules involving the neutral member of the isospin triplet, whose charge conjugation quantum number is $C = -G$.

There are some selection rules that follow from the exact symmetries of QCD. These symmetries include rotational symmetry, parity, and charge conjugation. We take the quantum numbers of the $Q\bar{Q}$ mesons before and after the transition to be J^{PC} and $J'^{P'C'}$. We consider a transition via the emission of a single hadron h with quantum numbers $J_h^{P_h C_h}$ in

a state with orbital-angular-momentum quantum number L_h. The conservation of parity and charge conjugation imply the selection rules

$$P = P' P_h (-1)^{L_h}, \tag{25a}$$
$$C = C' C_h. \tag{25b}$$

Angular momentum conservation requires J to be in the range between $|J' - (J_h + L_h)|$ and $J' + (J_h + L_h)$.

The remaining selection rules for hadronic transitions are only approximate. There is a *spin selection rule* that follows from the approximate heavy-quark spin symmetry:

$$S = S', \tag{26}$$

where S and S' are the total spin quantum numbers for the $Q\bar{Q}$ pair before and after the transition. Transitions between spin-singlet and spin-triplet states have rates that are suppressed by the square of the ratio of a hadronic scale to the heavy quark mass. Since m_b is about 3 times larger than m_c, this suppression factor is an order of magnitude smaller for $b\bar{b}$ mesons than for $c\bar{c}$ mesons.

There are also *Born-Oppenheimer selection rules* that constrain the quantum numbers Λ_η^ϵ of the light-field configurations of the $Q\bar{Q}$ mesons involved in the hadronic transition [39]. Since the time scale for evolution of the gluon and light-quark fields is much faster than that for the motion of the Q and $\bar{Q}$, the emission of light hadrons can proceed through an almost instantaneous transition of the light-field configuration, with the positions of the Q and $\bar{Q}$ remaining essentially fixed. We consider a transition via the emission of a single hadron h with quantum numbers $J_h^{P_h C_h}$. The light-field configurations can be labelled by the separation vector $\boldsymbol{r}$ of the Q and $\bar{Q}$ and by the quantum numbers introduced in Section III B: the eigenvalues Λ, η, and ϵ of $|\boldsymbol{r} \cdot \boldsymbol{J}_{\rm light}|$, $(CP)_{\rm light}$, and $R_{\rm light}$, respectively. The flavor-singlet configurations can be denoted by kets $|\Lambda, \eta, \epsilon\,; \boldsymbol{r}\rangle$. For $\Lambda \geq 1$, these kets are linear combination of eigenstates of $\boldsymbol{r} \cdot \boldsymbol{J}_{\rm light}$ with eigenvalues $\lambda = \pm\Lambda$. A hadronic transition between flavor-singlet light-field configurations in which the hadron h is emitted with momentum $\boldsymbol{q}$ can be expressed as

$$\big|\Lambda, \eta, \epsilon\,; \boldsymbol{r}\big\rangle \longrightarrow \big|\Lambda', \eta', \epsilon\,; \boldsymbol{r}\big\rangle \big|h(\boldsymbol{q})\big\rangle. \tag{27}$$

The conservation of the component of the total angular momentum $\boldsymbol{J}_{\rm light}$ of the light fields along the $Q\bar{Q}$ axis can be expressed as

$$\lambda = \lambda' + \hat{\boldsymbol{r}} \cdot (\boldsymbol{J}_h + \boldsymbol{L}_h), \tag{28}$$

where $\boldsymbol{J}_h$ and $\boldsymbol{L}_h$ are the spin vector and orbital-angular-momentum vector of the light hadron h. If h is emitted with orbital-angular-momentum quantum number L_h, the constraint in Eq. (28) implies the selection rule

$$|\lambda - \lambda'| \leq J_h + L_h. \tag{29}$$

The quantum numbers η and η' in Eqs. (27) are the eigenvalues of $(CP)_{\rm light}$ for the light-field configurations. Conservation of $(CP)_{\rm light}$ implies the selection rule

$$\eta = \eta' \cdot C_h P_h (-1)^{L_h}. \tag{30}$$

In the special case $\lambda = \lambda' = 0$, there is an additional constraint from invariance under reflection through a plane containing the $Q\bar{Q}$ axis. The initial and final light-field configurations $|0, \eta, \epsilon\,; \boldsymbol{r}\rangle$ and $|0, \eta', \epsilon'\,; \boldsymbol{r}\rangle$ are eigenstates of the reflection operator $R_{\rm light}$ with eigenvalues ϵ and ϵ', respectively. The effect of the reflection on the emitted hadron can be deduced by expressing $R_{\rm light}$ as the product of the parity operator $P_{\rm light}$ and a rotation by angle π around the axis of the reflection plane. Such a rotation changes the phase by $\exp(i\pi\hat{\boldsymbol{r}} \cdot (\boldsymbol{J}_h + \boldsymbol{L}_h))$, which equals 1 by the constraint in Eq. (28). The additional constraint imposed by the reflection symmetry is therefore

$$\epsilon = \epsilon' \cdot P_h (-1)^{L_h} \qquad (\lambda = \lambda' = 0). \tag{31}$$

The hadronic transitions are also governed by flavor selection rules associated with conservation of net light-quark flavors. We will only consider hadronic transitions in which the final $Q\bar{Q}$ meson is a quarkonium. Since it is a flavor singlet, the flavor selection rules are trivial.

E. Candidates for XYZ mesons

Many of the hadronic transitions of the XYZ mesons listed in Tables I, II, and III are to quarkonium states. For $c\bar{c}$ mesons, the charmonium states are the spin-triplet 1^{--} states J/ψ and $\psi(2S)$, the spin-triplet 1^{++} state $\chi_{c1}(1P)$, and the spin-singlet 1^{+-} state $h_{c1}(1P)$. For $b\bar{b}$ mesons, the bottomonium states are the spin-triplet 1^{--} states $\Upsilon(nS)$ and the spin-singlet 1^{+-} states $h_{c1}(nP)$.

When applied to the $c\bar{c}$ mesons listed in Tables I and II, the spin selection rule implies that the only plausible candidates for XYZ mesons with transitions to J/ψ, $\psi(2S)$, or $\chi_{cJ}(1P)$ are spin-triplet members of charmonium hybrid or charmonium tetraquark multiplets. The only plausible candidates for XYZ mesons with transitions to $h_c(1P)$ are spin-singlet members of charmonium hybrid or charmonium tetraquark multiplets. The spin selection rule puts strong constraints on the interpretations of the XYZ mesons in Table I with quantum numbers 1^{--}. In the quarkonium hybrid multiplets listed in Table V, the only 1^{--} states are the spin-singlet members of the $\Pi_u^+(1P)$ and $\Sigma_u^-(1P)$ multiplets. In the quarkonium tetraquark multiplets listed in Table V, there is a spin-singlet 1^{--} state in the $\Sigma_u^-(1P)$ multiplet and there are spin-triplet 1^{--} states in the $\Pi_g^-(1D)$, $\Pi_g^+(1P)$, $\Sigma_g^+(1S)$, and $\Sigma_g^+(1D)$ multiplets. The 1^{--} $c\bar{c}$ meson $Y(4220)$ in Table I, which decays into $h_c(1P)\,\pi^+\pi^-$ [14], must be a spin-singlet. If we assume that the $Y(4220)$ is the ground state of a B-O potential, it can only be identified with the 1^{--} state in the $\Pi_u^+(1P)$ energy level of the charmonium hybrid. The 1^{--} $c\bar{c}$ meson $Y(4260)$ in Table I, which decays into $J/\psi\,\pi^+\pi^-$ [2], must be a spin-triplet. If we assume that the $Y(4260)$ is the ground state in a B-O potential, it can be identified with the 1^{--} state in either the $\Pi_g^+(1P)$ or $\Sigma_g^+(1S)$ energy level of the isospin-0 charmonium tetraquark.

When applied to the $b\bar{b}$ mesons listed in Table III, the spin selection rule presents a puzzle. The $Z_b^+(10610)$ and $Z_b^+(10650)$ have hadronic transitions to both the spin-triplet bottomonium states $\Upsilon(nS)$ and the spin-singlet bottomonium states $h_b(nS)$ [4]. Thus their decays violate the spin selection rule. This can be explained by the $Z_b^+(10610)$ having a large $B^*\bar{B}$ molecular component and the $Z_b^+(10650)$ having a large $B^*\bar{B}^*$ molecular component [36–38]. Within the Born-Oppenheimer approach, the large molecular components would arise from energy levels in B-O potentials that are fortuitously close to the $B^*\bar{B}$ and $B^*\bar{B}^*$ thresholds, which results in a breakdown of the single-channel approximation.

Several of the hadronic transitions for the neutral $c\bar{c}$ mesons listed in Table I are the emission of a single vector meson ω or ϕ with $J_h^{P_h C_h} = 1^{--}$. Since the kinetic energy of the vector meson is small compared to its mass, we assume it is emitted in an S-wave state. The B-O selection rules in Eqs. (29), (30), and (31) reduce to $|\lambda - \lambda'| \leq 1$, $\eta = \eta'$, and also $\epsilon = -\epsilon'$ if $\lambda = \lambda' = 0$. If the final-state configuration is Σ_g^+ corresponding to a quarkonium, the selection rules reduce further to $\Lambda \leq 1$, $\eta = +1$, and also $\epsilon = -1$ if $\Lambda = 0$. They imply that the only possible initial-state configurations are Π_g^-, Π_g^+, and Σ_g^-. The quarkonium hybrid configurations with the deepest potentials are Π_u^+, Π_u^-, and Σ_u^-. None of these can make a transition to quarkonium through the S-wave emission of a vector meson. The quarkonium tetraquark configurations with the deepest potentials are presumably Π_g^-, Π_g^+, Σ_g^+, and Σ_u^-. Of these, the only ones that can make a transition to quarkonium through the S-wave emission of a vector meson are Π_g^- and Π_g^+. We first consider the $X(3915)$, which decays into $J/\psi\,\omega$ and has quantum numbers 0^{++} [40]. In the Π_g^- and Π_g^+ tetraquark multiplets listed in Table V, the only 0^{++} state is a spin-triplet member of $\Pi_g^-(1P)$. We therefore identify $X(3915)$ with the 0^{++} member of the $\Pi_g^-(1P)$ multiplet of isospin-0 charmonium tetraquarks. We next consider the $Y(4140)$, $Y(4274)$, and $X(4350)$, which have $C = +$ and decay into $J/\psi\,\phi$. The ϕ in the final state suggests that the meson is an $s\bar{s}$ tetraquark. In the Π_g^- and Π_g^+ tetraquark multiplets listed in Table V, there are spin-triplet $C = +$ states in the multiplets $\Pi_g^-(1P)$, $\Pi_g^-(1F)$, and $\Pi_g^+(1D)$. If we assume that the lowest of these three states, $Y(4140)$, is in the ground state of a B-O potential, it must be the 0^{++}, 1^{++}, or 2^{++} member of the $\Pi_g^-(1P)$ multiplet of $s\bar{s}$ charmonium tetraquarks. The energy difference of about 230 MeV between the $Y(4140)$ and the $X(3915)$ is approximately twice the difference between the constituent masses of an s quark and a lighter quark. It is therefore compatible with the identifications of $Y(4140)$ and $X(3915)$ as states in the $\Pi_g^-(1P)$ multiplets of $s\bar{s}$ and isospin-0 charmonium tetraquarks, respectively.

The hadronic transitions for the charged $c\bar{c}$ mesons listed in Table II and for the charged $b\bar{b}$ mesons listed in Table III are the emission of a single π^+ with $J_h^{P_h C_h} = 0^{-+}$. The Goldstone nature of the pion requires that it be emitted in a P-wave state. The B-O selection rules in Eqs. (29), (30), and (31) reduce to $|\lambda - \lambda'| \leq 1$, $\eta = \eta'$, and also $\epsilon = \epsilon'$ if $\lambda = \lambda' = 0$. If the final-state configuration is Σ_g^+ corresponding to a quarkonium, the selection rules reduce further to $\Lambda \leq 1$, $\eta = +1$, and also $\epsilon = +1$ if $\Lambda = 0$. They imply that the only possible initial-state configurations are Π_g^-, Π_g^+, and Σ_g^+. Isospin symmetry provides the additional selection rule that the initial configuration must have isospin 1. The quarkonium tetraquark configurations with the deepest potentials are presumably Π_g^-, Π_g^+, Σ_g^+, and Σ_u^-. The only ones that can make a transition to quarkonium through the P-wave emission of a pion are Π_g^-, Π_g^+, and Σ_g^+. The $Z_c^+(3900)$ decays into $J/\psi\,\pi^+$ [5]. Its neutral isospin partner $Z_c^0(3900)$ has $C = -$. The Π_g^-, Π_g^+, and Σ_g^+ tetraquark multiplets listed in Table V include many spin-triplet $C = -$ states. If we assume the $Z_c^0(3900)$ is in the ground state of a B-O potential, it must be the 0^{--}, 1^{--}, or 2^{--} state in the $\Pi_g^+(1P)$ multiplet or the 1^{--} state in the $\Sigma_g^+(1S)$ multiplet of isospin-1 charmonium tetraquarks. The $Z_c^+(4020)$ decays into $h_c(1P)\,\pi^+$ [18]. Its neutral isospin partner $Z_c^0(4020)$ has $C = -$. In the Π_g^-, Π_g^+, and Σ_g^+ tetraquark multiplets listed in Table V, the spin-singlet $C = -$ states are in the $\Pi_g^-(1P)$, $\Pi_g^-(1F)$, $\Pi_g^+(1D)$, and $\Sigma_g^+(1P)$ multiplets. If we assume the $Z_c^0(4020)$ is in the ground state of a B-O potential, it must be the 1^{+-} state in the $\Pi_g^-(1P)$ multiplet of isospin-1 charmonium tetraquarks. The $Z_1^+(4050)$ and $Z_2^+(4250)$ decay into $\chi_{c1}(1P)\,\pi^+$ [41]. Their neutral isospin partners $Z_1^0(4050)$ and $Z_2^0(4250)$ have $C = +$. The Π_g^-, Π_g^+, and Σ_g^+ tetraquark multiplets listed in Table V include many spin-triplet $C = +$ states. If we assume the $Z_1^0(4050)$ is in

the ground state of a B-O potential, it must be the 0^{++}, 1^{++}, or 2^{++} state in the $\Pi_g^-(1P)$ multiplet of isospin-1 charmonium tetraquarks. The small difference between the masses of $Z_c^+(4020)$ and $Z_1^+(4050)$ is compatible with their being different states in the $\Pi_g^-(1P)$ multiplet of isospin-1 charmonium tetraquarks.

Finally, we consider the implications of the B-O selection rules in Eqs. (29), (30), and (31) for the only neutral $b\bar{b}$ XYZ meson listed in Table III. The $Y(10890)$ has quantum numbers 1^{--}, and it has been observed in the decay channel $\Upsilon(nS)\,\pi^+\pi^-$[42]. If this state is a ground-state energy level of a B-O potential, the only bottomonium hybrid option is the spin-singlet 1^{--} state in the $\Pi_u^+(1P)$ multiplet. The bottomonium tetraquark options are the spin-triplet 1^{--} state in either the $\Pi_g^+(1P)$ multiplet or the $\Sigma_g^+(1S)$ multiplet. The decays of $Y(10890)$ into $\Upsilon(nS)\,\pi^+\pi^-$ favors one of the spin-triplet options. However these decays may have large contributions from direct decays into $Z_b(10610)\,\pi$ and $Z_b(10650)\,\pi$, followed by the subsequent decay of the Z_b meson into $\Upsilon(nS)\,\pi$. The $Z_b(10610)$ and $Z_b(10650)$ also decay into $h_b(nP)\,\pi$. Hadronic transitions of the Z_b mesons to both the spin-triplet bottomonium states $\Upsilon(nS)$ and the spin-singlet bottomonium states $h_b(nP)$ violate the spin selection rule. In order to determine the implications of the B-O selection rules for the $Y(10890)$, we would first need to determine whether its direct decays obey the spin selection rule.

V. LATTICE GAUGE THEORY

In this section, we describe the existing results on the spectra of hybrid and tetraquark $c\bar{c}$ and $b\bar{b}$ mesons that have been calculated using lattice gauge theory. They provide some information about the pattern of deviations from the Born-Oppenheimer approximation.

A. Charmonium hybrids from lattice QCD

The spectrum of charmonium hybrids can be calculated directly using lattice QCD. Exploratory calculations of the $c\bar{c}$ meson spectrum above the open-charm threshold were carried out by Dudek, Edwards, Mathur, and Richards [43] and extended by the Hadron Spectrum Collaboration [44]. The most recent published calculations used an anisotropic lattice with $24^3 \times 128$ sites and a spatial lattice spacing of about 0.12 fm. Their gauge field configurations were generated using dynamical u, d, and s quarks, with the s quark having its physical mass and the u and d quarks unphysically heavy, corresponding to a pion mass of about 400 MeV. On a cubic lattice, there are 20 channels analogous to the J^{PC} quantum numbers in the continuum. For each of the 20 lattice J^{PC} channels, the Hadron Spectrum Collaboration calculated the $c\bar{c}$ meson spectrum from the Euclidean time dependence of the cross-correlators for a set of operators whose number ranged from 4 to 26, depending on the channel. The operators included "hybrid" operators constructed out of the c quark field and the gluon field strength and "charmonium" operators constructed out of the c quark field and other combinations of covariant derivatives.

The Hadron Spectrum Collaboration identified 46 states in the $c\bar{c}$ meson spectrum with high statistical precision [44]. These states had spins J as high as 4 and masses as high as 4.6 GeV. The states that are more strongly excited by hybrid operators are plausible candidates for charmonium hybrids. All the charmonium hybrid candidates in the calculations

multiplet	Γ	nL	$\langle\text{energy}\rangle_{\text{spin}}$	J^{PC}	$c\bar{c}$ hybrids lattice QCD
H_1	Π_u^+	$1P$	4212 ± 22	1^{--}	$\mathbf{(4216 \pm 7)}$
				0^{-+}	4126 ± 20
				$\mathbf{1}^{-+}$	4148 ± 22
				2^{-+}	4265 ± 23
H_2	Π_u^-	$1P$	4314 ± 32	1^{++}	4330 ± 21
				$\mathbf{0}^{+-}$	4317 ± 18
				1^{+-}	4275 ± 41
				$\mathbf{2}^{+-}$	4326 ± 43
H_3	Σ_u^-	$1S$	4407 ± 22	0^{++}	4403 ± 34
				1^{+-}	4408 ± 25
H_4	Π_u^+	$1D$	4448 ± 19	2^{++}	4423 ± 26
				1^{+-}	4428 ± 42
				$\mathbf{2}^{+-}$	4443 ± 24
				3^{+-}	4479 ± 20

TABLE VI: Charmonium hybrid energies (in MeV) predicted using the splittings between states calculated using lattice QCD in Ref. [44]. The experimental input in parentheses is the measured mass of the $Y(4220)$, which is identified as the 1^{--} hybrid in the ground-state H_1 multiplet. The column labelled $\langle\text{energy}\rangle_{\text{spin}}$ gives the spin-averaged energies of the multiplets. The error bars take into account the statistical errors in the lattice calculations. They do not account for systematic errors associated with extrapolations to zero lattice spacing and to the physical u and d quark masses.

of Ref. [44] can be organized into four complete heavy-quark spin-symmetry multiplets:

$$H_1 = \{1^{--}, (0, \mathbf{1}, 2)^{-+}\}, \tag{32a}$$
$$H_2 = \{1^{++}, (\mathbf{0}, 1, \mathbf{2})^{+-}\}, \tag{32b}$$
$$H_3 = \{0^{++}, 1^{+-}\}, \tag{32c}$$
$$H_4 = \{2^{++}, (1, \mathbf{2}, 3)^{+-}\}. \tag{32d}$$

A bold $\boldsymbol{J}$ indicates that $\boldsymbol{J}^{PC}$ is an exotic quantum number that is not possible if the constituents are only $Q\bar{Q}$. If we consider only the central values of the energies of the states, the ordering in energies of the multiplets from lowest to highest are H_1, H_2, H_3, and H_4. If we take into account the statistical errors in the energies, there may be small overlaps between some of the multiplets. The calculations in Ref. [44] are not definitive, because they were not extrapolated to zero lattice spacing or to the physical values of the u and d quark masses. However since light quarks are not expected to be important as constituents in charmonium or in charmonium hybrids, the results of Ref. [44] provide plausible estimates for the masses of the charmonium hybrids. The energy splittings between charmonium hybrid states may be less sensitive to the effects of light quarks than their masses.

In Ref. [11], the $Y(4260)$ was identified as the lowest 1^{--} charmonium hybrid. The masses of other charmonium hybrids were then estimated by using the results of Ref. [44] for the splittings between $c\bar{c}$ mesons. This identification was motivated primarily by the very

small cross section for producing the $Y(4260)$ in e^+e^- annihilation, despite it having the appropriate quantum numbers 1^{--}. The small cross section can be explained by the small wavefunction for $c\bar{c}$ at the origin that is characteristic of a quarkonium hybrid. The only 1^{--} state among the charmonium hybrid multiplets in Eqs. (32) is the spin-singlet member of H_1. But an important decay mode of the $Y(4260)$ is the discovery channel $J/\psi\,\pi^+\pi^-$, which is a spin-triplet decay channel. The identification of the $Y(4260)$ with this state is therefore disfavored by the spin selection rule, which requires a spin-singlet charmonium hybrid to decay preferentially into spin-singlet charmonium states.

The BESIII Collaboration has recently observed the $Y(4220)$, which has quantum numbers 1^{--} and decays into $h_c\,\pi^+\pi^-$, which is a spin-singlet decay channel. The $Y(4220)$ can plausibly be identified with the spin-singlet member of the H_1 multiplet. We therefore identify the $Y(4220)$ as the 1^{--} member of the ground-state charmonium hybrid multiplet. The masses of other charmonium hybrids are then estimated by using the results of Ref. [44] for the splittings between $c\bar{c}$ mesons. The results are shown in Table VI. The errors are statistical uncertainties only. They do not include the systematic errors associated with the extrapolation to zero lattice spacing or to the small physical masses of the u and d quarks.

The Born-Oppenheimer interpretations of the multiplets H_1, H_2, H_3, and H_4 in Eqs. (32) are the $\Pi_u^+(1P)$, $\Pi_u^-(1P)$, $\Sigma_u^-(1S)$, and $\Pi_u^+(1D)$ energy levels, respectively. The results in Table VI give us some idea of the size of corrections to the B-O approximation. In the leading B-O approximation, the Π_u potential is the same for $\epsilon = +1$ and -1. However the spin average for the $\Pi_u^-(1P)$ multiplet is about 100 MeV higher than the spin average for the $\Pi_u^+(1P)$ multiplet. In the leading B-O approximation, the states in each spin-symmetry multiplet are degenerate. However the range of energies within the H_1 multiplet is about 140 MeV and the ranges of energies within the H_2 and H_4 multiplets are about 60 MeV. The $\Pi_u^+(1P)$ and $\Pi_u^+(1D)$ energy levels are the ground state and the first orbital-angular-momentum excitation of the Π_u^+ configuration. The splitting of 240 MeV between their spin averages can be used as an estimate for orbital-angular-momentum splittings.

An alternative interpretation of the lowest charmonium hybrid spin-symmetry multiplets can be obtained by interpreting the 1^{+-} ground-state gluelump as a constituent gluon with no orbital angular momentum bound to a color-octet heavy quark-antiquark pair. If the $Q\bar{Q}$ pair is in an S-wave state, its spin-symmetry multiplet is $\{0^{-+}, 1^{--}\}$. The spin-symmetry multiplet of the hybrid meson is then $1^{+-} \otimes \{0^{-+}, 1^{--}\}$, which is equivalent to $H_1 = \{1^{--}, (0, \mathbf{1}, 2)^{-+}\}$. Thus the ground-state gluelump bound to an S-wave $Q\bar{Q}$ pair gives rise to the same spin-symmetry multiplet as the ground-state $Q\bar{Q}$ hybrid. If the $Q\bar{Q}$ pair is in a P-wave state, its spin-symmetry multiplet is $\{1^{+-}, (0, 1, 2)^{++}\}$. The spin-symmetry supermultiplet of the hybrid mesons is then $1^{+-} \otimes \{1^{+-}, (0, 1, 2)^{++}\}$. The spin-singlet states are $(0, 1, 2)^{++}$ and the spin-triplet states are $(\mathbf{0}, 1, 1, 1, \mathbf{2}, \mathbf{2}, 3)^{+-}$. They account for all the states in H_2, H_3, and H_4. Dudek has argued that the first excited energy levels of a light-quark hybrid form such a supermultiplet [45]. For the charmonium hybrid energy levels in Table VI, the range of energies for the complete supermultiplet consisting of H_2, H_3, and H_4 is about 200 MeV, while the ranges of energies within the individual multiplets H_2, H_3, and H_4 are about 55, 5, and 56 MeV, respectively. This suggest that the Bonn-Oppenheimer interpretation provides a more useful first approximation than the constituent gluelump interpretation.

B. Bottomonium hybrids from lattice NRQCD

The mass of the bottom quark is too large for lattice QCD with a conventional isotropic lattice to be applied directly to $b\bar{b}$ mesons with currently available computational resources. One alternative is to use an anisotropic lattice in which the lattice spacing is much finer in the Euclidean time direction than in the three spacial directions. Another alternative is to use a lattice discretization of an effective field theory called *NonRelativistic QCD* (NRQCD) in which the b quark is treated nonrelativistically [46]. This method can also be applied to $c\bar{c}$ mesons, although the errors associated with the nonrelativistic approximation are larger.

Quenched lattice NRQCD was used by Juge, Kuti, and Morningstar to calculate the masses of some of the states in the $b\bar{b}$ meson spectrum [13]. They used a lattice NRQCD action that included only the leading terms in the velocity expansion, which gives no spin splittings within spin-symmetry multiplets. They used a lattice with $15^3 \times 45$ sites and a spatial lattice spacing of about 0.12 fm. For each of 5 lattice J^{PC} channels, they calculated the $b\bar{b}$ meson spectrum from the Euclidean time dependence of the cross-correlators for either 1 or 4 operators. The states that are more strongly excited by hybrid operators are plausible candidates for bottomonium hybrids. They identified four candidate bottomonium hybrid states. The three lowest-energy states were the 1^{--}, 1^{++}, and 0^{++} members of the lowest three spin-symmetry multiplets H_1, H_2, and H_3 defined in Eq. (32). The fourth and highest-energy state, which has quantum numbers 1^{--}, can be interpreted as a radial excitation of the ground-state quarkonium hybrid. The corresponding multiplet is labelled H_1'. Candidates for such a multiplet were not observed in the lattice QCD calculations of charmonium hybrids in Ref. [44]. The reason for this could be that the operators used to excite charmonium hybrids in Ref. [44] did not couple sufficiently strongly to radial excitations. The difference of about 440 MeV between the masses of the 1^{--} states in the H_1' and H_1 multiplets can be used as an estimate for splittings between radial excitations.

Liao and Manke have calculated the $b\bar{b}$ meson spectrum using quenched lattice QCD on an anisotropic lattice [47]. They used a lattice with $16^3 \times 128$ sites, with a spacial lattice spacing of 0.05 fm and a much finer lattice spacing in the Euclidean time direction. They determined the masses for three $b\bar{b}$ hybrid mesons with exotic quantum numbers from the Euclidean time dependence of the correlators of appropriate operators. The $\mathbf{1}^{-+}$ state is a member of the H_1 multiplet, while the $\mathbf{0}^{+-}$ and $\mathbf{2}^{+-}$ states are members of the H_2 multiplet.

Since the lattice calculations in Refs. [13] and [47] do not include the effects of light-quark loops, any quantitative predictions should be treated with caution. Nevertheless, we proceed to use the results to estimate the energy levels for bottomonium hybrids. In the lattice NRQCD calculations of Ref. [13], the lattice energy scale cancels out in the ratios of the energy splittings of the bottomonium hybrids to the $1P - 1S$ splitting of bottomonium. We therefore determine the energy splittings by multiplying the ratios by the observed $1P - 1S$ splitting of bottomonium. To determine the absolute energies of the bottomonium hybrids in the lattice NRQCD calculation, we need an experimental input to determine the energy offset. We arbitrarily choose the mass of the 1^{--} member of the ground-state H_1 multiplet to be the $B\bar{B}$ threshold, which is 10559 MeV. The splittings from Ref. [13] are then used to estimate the masses of other bottomonium hybrids, which are given in Table VII. To determine the absolute energies of the bottomonium hybrids in the lattice QCD calculation, we arbitrarily choose the mass of the $\mathbf{1}^{-+}$ member of the ground-state H_1 multiplet to be the $B\bar{B}$ threshold. The splittings from Ref. [47] are then used to estimate the masses of other bottomonium hybrids, which are given in Table VII. The error bars in Table VII

multiplet	Γ	nL	J^{PC}	$b\bar{b}$ hybrids lattice NRQCD	$b\bar{b}$ hybrids lattice QCD
H_1	Π_u^+	$1P$	1^{--}	(10559)	
			$\mathbf{1}^{-+}$		(10559)
H_2	Π_u^-	$1P$	1^{++}	10597 ± 65	
			$\mathbf{0}^{+-}$		10159 ± 362
			$\mathbf{2}^{+-}$		11323 ± 257
H_3	Σ_u^-	$1S$	0^{++}	10892 ± 36	
H_1'	Π_u^+	$2P$	1^{--}	10977 ± 41	

TABLE VII: Bottomonium hybrid energies (in MeV) predicted using the splittings between states calculated using quenched lattice NRQCD in Ref. [13] and using quenched lattice QCD in Ref. [47]. The inputs in parentheses for the $\Pi_u^+(1P)$ energy levels have been chosen arbitrarily to be the $B\bar{B}$ threshold. The error bars take into account the statistical errors in the lattice calculations and the uncertainties from setting the heavy-quark mass. They do not account for systematic errors associated with extrapolations to zero lattice spacing and from the omission of light quark loops.

take into account the statistical errors in the lattice calculations and the uncertainties from setting the heavy-quark mass. They do not account for systematic errors associated with extrapolations to zero lattice spacing and from the omission of light-quark loops. The error bars in the mass splittings from the lattice QCD calculation are much larger than those from the lattice NRQCD calculation. They are comparable to the splitting between the H_1 and H_3 multiplets.

We can compare the mass splittings for bottomonium hybrids in Table VII calculated using quenched lattice NRQCD with the mass splittings for charmonium hybrids in Table VI calculated using lattice QCD with dynamical light quarks. The central value of the splitting between the 1^{++} state of H_2 and the 1^{--} state of H_1 for bottomonium hybrids is about 1/3 that for charmonium hybrids. The central value of the splitting between the 0^{++} state of H_3 and the 1^{--} state of H_1 for bottomonium hybrids is about twice as large as that for charmonium hybrids. Definitive calculations of the spectrum of bottomonium hybrids using lattice NRQCD with dynamical light quarks would be valuable.

C. Charmonium tetraquarks from lattice QCD

Lattice QCD has not yet provided much information on quarkonium tetraquarks. Pelovsek and Leksovec have made a first attempt to observe the charmonium tetraquark $Z_c(3900)$ using lattice QCD with dynamical u and d quarks under the assumption that its $I^G(J^P)$ quantum numbers are $1^+(1^+)$ [48]. They looked for a signal for the Z_c in the cross correlators of 6 operators. Three of the operators were linear combinations of products of color-singlet $c\bar{q}$ and $q\bar{c}$ operators, so they couple most strongly to states that consist of a pair of charm mesons $D^*\bar{D}$. The other 3 operators were linear combinations of products of color-singlet $c\bar{c}$ and $q\bar{q}$ operators, so they couple most strongly to states that consist of $J/\psi\,\pi$. The only signals they observed were for scattering states of the meson pairs $D^*\bar{D}$ and $J/\psi\,\pi$.

In the Born-Oppenheimer picture, the component of a charmonium tetraquark in which the $c\bar{c}$ pair is close together can be approximated by a charmonium adjoint meson, which consists of a light $q\bar{q}$ pair bound to a color-octet $c\bar{c}$ pair. This suggests that the operators that couple most strongly to charmonium tetraquarks could be linear combinations of products of a color-octet $c\bar{c}$ operator and a color-octet $q\bar{q}$ operator. Such operators would have suppressed couplings to scattering states consisting of a pair of mesons. Operators with this structure should be included in a comprehensive study of charmonium tetraquarks in lattice QCD.

D. Quarkonium hybrids from QCD sum rules

Numerous papers have been written in which QCD sum rules are used to postdict the masses of individual XYZ mesons in Tables I, II, and III. A global analysis of the pattern of XYZ states predicted by QCD sum rules would be more useful. Such an analysis has been carried out for charmonium hybrids and bottomonium hybrids by Chen *et al.* [49]. They identified a total of 10 hybrid states, with the same pattern of masses for charmonium hybrids and bottomonium hybrids. The states with the four lowest masses are those in the multiplet H_1 in Eq. (32a). The five states with the next higher masses have quantum numbers that correspond to 5 of the 8 states in the multiplets H_2, H_3, and H_4 in Eqs. (32). The highest-mass state identified in Ref. [49] had the exotic quantum numbers $\mathbf{0}^{--}$. In the Born-Oppenheimer approach, the lowest $\mathbf{0}^{--}$ quarkonium hybrid could be a spin-triplet state in the first orbital-angular-momentum excitation of the Σ_g^- hybrid potential. It is useful to compare the QCD sum rule predictions for charmonium hybrids with those from lattice QCD in Table VI. The lowest-mass state is predicted by QCD sum rules to be the 1^{--} state of H_1, while lattice QCD predicts it to be the 0^{-+} state of H_1. Lattice QCD predicts that the higher-mass states can be arranged into multiplets H_2, H_3, and H_4 with increasing masses. QCD sum rules do not predict any such ordering of the masses in the three multiplets. A $\mathbf{0}^{--}$ charmonium hybrid was not observed in the lattice QCD calculations of Ref. [44].

VI. PHENOMENOLOGICAL ANALYSIS

In this section, we present predictions for energy levels of charmonium hybrids and bottomonium hybrids using the Born-Oppenheimer approximation in conjunction with inputs from lattice gauge theory. We also present a speculative illustration of some of the energy levels of charmonium tetraquarks.

A. Quarkonium

A crucial parameter in the B-O approximation is the heavy-quark mass m_Q, which appears in the radial Schroedinger equation in Eq. (21). If there was a rigorous derivation of the B-O approximation as the leading term in a systematic approximation to QCD, it would be possible to determine the appropriate value of m_Q from the parameters of QCD. In the absence of such a derivation, an alternative is to treat the charm quark mass m_c and the bottom quark mass m_b as phenomenological parameters. Since we wish to determine the energy levels of quarkonium hybrids and quarkonium tetraquarks by solving the

	charmonium	bottomonium
$1S$	3067.9 ± 0.3	9445.0 ± 0.7
$1P$	3525.3 ± 0.1	9899.9 ± 0.4
$2S$	3674.3 ± 0.3	10017.2 ± 1.1
$2P$		10260.2 ± 0.5
m_Q (GeV)	1.48	4.89
σ (GeV^2)	0.187	
κ	0.489	
V_0 (GeV)	-0.242	

TABLE VIII: Spin-averaged energy levels (in MeV) for charmonium and bottomonium multiplets and the parameters of the Cornell potential obtained by fitting those energies with the constraint $m_b - m_c = 3412.2$ MeV.

Schroedinger equation, we choose to determine m_c and m_b by fitting the quarkonium energy levels predicted by the Schroedinger equation in the Σ_g^+ potential to the measured energy levels of charmonium and bottomonium.

The energy levels E_{nL} for quarkonium are eigenvalues of the radial Schroedinger equation in Eq. (21) with potential $V_{\Sigma_g^+}(r)$ and with $\Lambda = 0$ and $J_\Gamma = 0$. The Σ_g^+ potential has been calculated using lattice QCD. An obvious way to determine m_Q is to solve the Schroedinger equation for that potential and then fit the single parameter m_Q to the observed quarkonium energy levels. One problem with this procedure is there are strong correlations between m_Q and the parameters of the potential. These parameters include the string tension σ, which determines the flavor-singlet B-O potentials at large r by Eq. (7). The value of σ from lattice QCD has a 10% error, and this limits the accuracy of the determination of m_Q. To deal with this problem, we will approximate the Σ_g^+ potential by the Cornell potential in Eq. (5) and determine the quark masses m_c and m_b as well as the parameters of the potential, including σ, by fitting the observed energy levels of charmonium and bottomonium. The fitted value of σ will then be used in the parametrization of the hybrid potentials. The energy levels of quarkonium hybrids will be obtained by solving the Schroedinger equation for those potentials with the fitted values of m_c and m_b.

The quarkonium energy levels in the Σ_g^+ potential are labeled by a radial quantum number $n = 1, 2, 3, \dots$ and by an orbital-angular-momentum quantum number $L = 0, 1, 2, \dots$ (or $S, P, D, \dots$). For each energy level nL, there are multiple states with different J^{PC} quantum numbers that are related by heavy-quark spin symmetry. The spin-symmetry multiplets for the $\Sigma_g^+(1S)$, $\Sigma_g^+(1P)$, and $\Sigma_g^+(1D)$ energy levels are given in Table V. Three complete charmonium multiplets below the $D\bar{D}$ threshold have been observed: $1S$, $1P$, and $2S$. Four complete bottomonium multiplets below the $B\bar{B}$ threshold have been observed: $1S$, $1P$, $2S$, and $2P$.

The Schrodinger equation in the Σ_g^+ potential predicts that the spin states in the multiplet for an energy level nL are all degenerate. Spin splittings arise from additional terms in the Hamiltonian that can be treated as perturbations. The energy levels in the Σ_g^+ potential can be interpreted as averages over the multiplet weighted by the number of spin states. The spin-averaged mass for the $1S$ energy level of charmonium, $\{\eta_c(1S), J/\psi\}$, is

$$M_{c\bar{c}(1S)} = \left(M_{\eta_c(1S)} + 3M_{J/\psi}\right)/4. \tag{33}$$

For all the observed P-wave multiplets, the mass of the spin-singlet 1^{+-} state is consistent with the spin-weighted average of the masses of the spin-triplet states 0^{++}, 1^{++}, and 2^{++}. A more precise value for the spin-weighted average mass for the multiplet can therefore be obtained by just using the spin-triplet states. Thus the spin-averaged mass for the $1P$ energy level of charmonium, $\{h_c(1P), (\chi_{c0}(1P), \chi_{c1}(1P), \chi_{c2}(1P))\}$, can be approximated by

$$M_{c\bar{c}(1P)} = \left(M_{\chi_{c0}(1P)} + 3M_{\chi_{c1}(1P)} + 5M_{\chi_{c2}(1P)}\right)/9. \tag{34}$$

The spin-averaged masses for the $1S$, $1P$, and $2S$ charmonium multiplets and the $1S$, $1P$, $2S$, and $2P$ bottomonium multiplets are given in Table VIII.

The Schroedinger equation for Q and $\bar{Q}$ interacting through the Cornell potential in Eq. (5) can be solved to obtain the energy levels E_{nL} as functions of the quark mass m_Q and the parameters σ, κ, and V_0. By dimensional analysis, the energy levels have the form

$$E_{nL}^{(Q)} = 2m_Q + V_0 + \left(\sigma^2/m_Q\right)^{1/3} \zeta_{nL}(\kappa(m_Q^2/\sigma)^{1/3}). \tag{35}$$

where $\zeta_{nL}(x)$ is a dimensionless function of its argument. The additive constant has been assumed to be the sum of $2m_Q$ and a term V_0 that is independent of the heavy quark. The splittings $E_{n'L'}^{(Q)} - E_{nL}^{(Q)}$ between energy levels depend only on the combinations of parameters σ^2/m_Q and $\kappa(m_Q^2/\sigma)^{1/3}$. Thus if we only fit the observed energy splittings, the heavy quark mass is completely arbitrary. Any change in m_Q can be compensated for all the energy splittings simultaneously by changes in σ and κ. One can determine $2m_Q + V_0$ by subsequently fitting one of the energy levels, such as the ground-state energy $E_{1S}^{(Q)}$. However, because $2m_Q + m_Q$ is determined by a single measurement only, it is more sensitive to the choice of the fitting observable than the combinations σ^2/m_Q and $\kappa(m_Q^2/\sigma)^{1/3}$.

By fitting observed splittings between charmonium energy levels and between bottomonium energy levels simultaneously, one can determine the combinations σ^2/m_b and $\kappa(m_b^2/\sigma)^{1/3}$ and the ratio m_b/m_c of the quark masses, but the individual quark mass m_b remains completely arbitrary. The individual quark masses and V_0 can be determined by subsequently fitting one of the charmonium energy levels and one of the bottomonium energy levels, such as the ground-state energies $E_{1S}^{(c)}$ and $E_{1S}^{(b)}$. However, because it is determined by two measurements only, m_b is more sensitive to the choice of the fitting observables than m_b/m_c, σ^2/m_b, and $\kappa(m_b^2/\sigma)^{1/3}$.

One way to decrease the sensitivity to the choice of fitting observables is to impose additional constraints on the quark masses. One such constraint is motivated by heavy quark symmetry, which implies that the mass of a heavy-light meson has an expansion in powers of $1/m_Q$. The leading term in the expansion is m_Q. The next-to-leading term of order m_Q^0 can be interpreted as the constituent mass of the light quark. This constituent quark mass cancels in the difference between the masses of a bottom meson and a charm meson with the same light flavor, leaving the difference between the quark masses. We choose to determine the quark mass difference from the difference between the average of the B^+ and B^0 masses and the average of the D^0 and D^+ masses:

$$m_b - m_c = m_B - m_D = 3412.2 \pm 0.2 \text{ MeV}. \tag{36}$$

We determine the parameters of the Cornell potential model by minimizing the χ^2 for the 7 spin-averaged energy levels for charmonium and bottomonium given in Table VIII, with the 7 energy levels equally weighted. The constraint in Eq. (36) is imposed on the quark

charmonium				bottomonium			
$n\,^{2S+1}L_J$	predicted	observed	difference	$n\,^{2S+1}L_J$	predicted	observed	difference
$1S$	3077	(3068)	+9	$1S$	9442	(9445)	−3
$1P$	3503	(3525)	−22	$1P$	9908	(9900)	+8
$2S$	3687	(3674)	+13	$2S$	10009	(10017)	−8
$1\,^3D_1$	3802	3773	+29	$1\,^3D_2$	10155	10164	−9
$2\,^3P_2$	3976	3927	+49	$2P$	10265	(10260)	+5
$3\,^3S_1$	4138	4039	+99	$3\,^3S_1$	10356	10355	+1
$2\,^3D_1$	4218	4153	+65				
$4\,^3S_1$	4525	4421	+104	$4\,^3S_1$	10638	10579	+59
				$5\,^3S_1$	10885	10876	+9
				$6\,^3S_1$	11110	11019	+91

TABLE IX: Energy levels (in MeV) for charmonium and bottomonium. The energy levels predicted by the Cornell potential with the parameters given in Table VIII are compared to the central values of the observed energy levels from Ref. [50]. The observed energy levels labelled nL are spin averaged. They are enclosed in parentheses, indicating that they were used as inputs to determine the parameters of the Cornell potential. The observed energy levels labelled $n\,^{2S+1}L_J$ are for individual spin states.

masses, so there only 4 independent parameters: σ, κ, V_0, and m_b. The resulting values of the parameters are given in Table VIII. The heavy quark masses are $m_c = 1.48$ GeV and $m_b = 4.89$ GeV. The constituent mass for the u and d quarks can be defined by the difference between m_B and m_b or between m_D and m_c, which are equal according to the constraint in Eq. (36). Using the fitted values for m_c or m_b, the constituent mass of the light quarks is 390 MeV. Solving the Schrodinger equation for the Cornell potential with the parameters given in Table VIII, we obtain predictions for all the energy levels of charmonium and bottomonium. The resulting predictions are compared with the observed energy levels in Table IX. For the spin-averaged energy levels used in the fit, the differences between the predicted and observed energy levels are at most 22 MeV. The highest energy levels in both the charmonium and bottomonium spectrum are underpredicted by about 100 MeV. The fitted value of the string tension in Table VIII, $\sigma = 0.187$ GeV^2, is compatible to within errors with the value 0.20 ± 0.02 GeV^2 determined by fitting lattice QCD calculations of the Σ_g^+ potential for two flavors of dynamical light quarks [27]. The fitted value κ= 0.489 in Table VIII is significantly larger than the value 0.368 obtained by fitting the lattice QCD calculations.

Heavy-quark spin symmetry implies that the mass splitting between the ground-state spin-triplet and spin-singlet mesons enters at order $1/m_Q$. This suggests that a more accurate constraint on the quark masses could be obtained by replacing m_D in Eq. (36) by the spin-weighted average of the spin-triplet mesons D^* and the spin-singlet mesons D and similarly for m_B. This would constrain the quark mass difference to be 3340.5 MeV. If this constraint is imposed instead of Eq. (36), the Cornell potential model gives a slightly better fit to the charmonium spectrum, and it gives a slightly worse fit to the bottomonium spectrum. However it gives much less reasonable values for the heavy quark masses: $m_c = 2.60$ GeV and $m_b = 5.94$ GeV. Given these fitted values of the heavy quark masses, the constituent

mass for the light quarks is negative. In light of this difficulty, we choose to use instead the constraint on the heavy quark masses in Eq. (36).

B. Hybrids

The energy levels of quarkonium hybrids in the B-O approximation can be calculated by solving the radial Schroedinger equation in Eq. (21) for the hybrid potentials. An accurate parametrization for the Π_u hybrid potentials calculated using quenched lattice QCD in Ref. [13] is given by Eq. (7) with $n_\Gamma = 1$ for $r > r_*$ and by Eq. (8) for $r < r_*$, along with the matching conditions at $r = r_*$ in Eqs. (10). An accurate parametrization of the difference between the Σ_u^- and Π_u hybrid potentials for $r < 2.4$ fm is given by Eq. (11). The parameter r_0 that appears in Eqs. (8) and (11) and in the matching conditions in Eqs. (10) is the Sommer radius defined by Eq. (6), which is determined from bottomonium spectroscopy to be $r_0 = 0.50$ fm. The string tension σ enters both potentials through the parametrization of the Π_u potential for $r > r_*$ in Eq. (7) and through the matching conditions at $r = r_*$ in Eqs. (10). We use the value $\sigma = 0.187$ GeV^2 in Table VIII, which was obtained by fitting the charmonium and bottomonium spectra. The matching point is then determined by Eq. (10b) to be $r_* = 1.5\ r_0$. The difference between the energy offsets is determined by Eq. (10a) to be $E_{\Pi_u} - E_0 = 2.6\ r_0^{-1}$.

Given our parametrizations of the Π_u and Σ_u^- potentials and given the quark masses $m_c = 1.48$ MeV and $m_b = 4.89$ MeV listed in Table VIII, the quarkonium hybrid energy levels can be obtained by solving the radial Schroedinger equation in Eq. (21). For charmonium hybrids, the ground-state $\Pi_u(1P)$ energy level is predicted to be 4246 MeV, and the $\Sigma_u^-(1S)$ energy level is predicted to be higher by 320 MeV. For bottomonium hybrids, the ground-state $\Pi_u(1P)$ energy level is predicted to be 10864 MeV, and the $\Sigma_u^-(1S)$ energy level is predicted to be higher by 233 MeV.

It is useful to compare the energy levels of charmonium hybrids in the B-O approximations with the spin-averaged energy levels from lattice QCD in Table VI. In the B-O approximation, the Π_u^+ and Π_u^- configurations have the same potential $V_{\Pi_u}(r)$, so they have the same energy levels. However the lattice QCD result in Table VI for the spin-averaged energy of the $H_2 = \Pi_u^-(1P)$ multiplet is about 100 MeV larger than that for the $H_1 = \Pi_u^+(1P)$ multiplet. With our parametrizations of the Π_u and Σ_u^- potentials, the $\Sigma_u^-(1S)$ energy level for charmonium hybrids is predicted to be higher than the $\Pi_u(1P)$ energy level by 320 MeV. However the lattice QCD result in Ref. [44] for the spin-averaged energy of the $H_3 = \Sigma_u^-(1S)$ multiplet is about 195 MeV higher than that for the $H_1 = \Pi_u^-(1P)$ multiplet.

The spectra of charmonium hybrids and bottomonium hybrids are illustrated in Figs. 2 and 3, respectively. Only the energy levels for the ground state, the first two orbital-angular-momentum excitations, and the first radial excitation in each potential are shown. To facilitate the comparison with later results, we have adjusted the energy offsets for the charmonium hybrids and bottomonium hybrids separately. For charmonium hybrids, we choose the offset so the $\Pi_u(1P)$ energy level is equal to 4212 MeV, which is the central value of the spin-averaged energy for the H_1 multiplet from lattice QCD given in Table VI. For bottomonium hybrids, we arbitrarily choose the offset so the $\Pi_u(1P)$ energy level is equal to the $B\bar{B}$ threshold, which is 10.559 GeV. The pattern of the energy levels for charmonium hybrids and bottomonium hybrids in Figs. 2 and 3 are quite similar. The orbital-angular-momentum splittings are smaller than the radial splittings. The energy splittings relative to the $\Pi_u(1P)$ energy level are smaller for bottomonium hybrids than for charmonium hybrids.

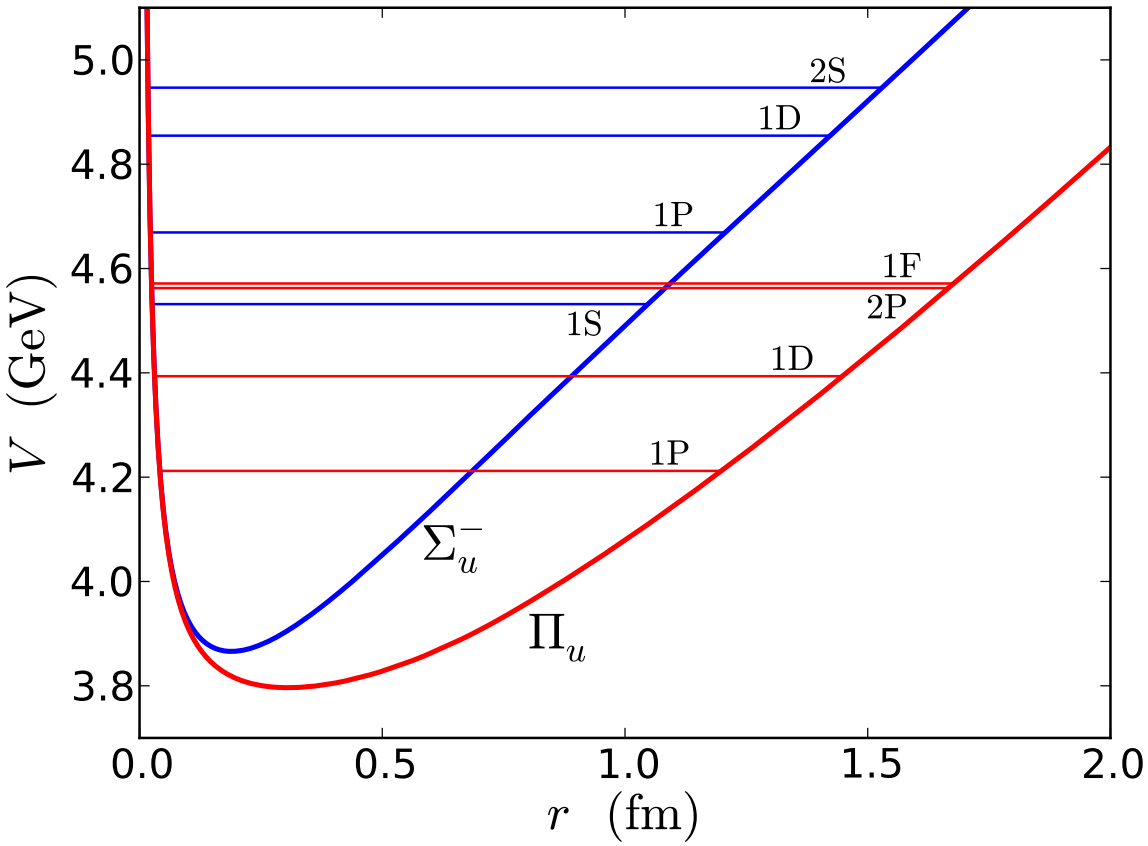

FIG. 2: Lowest energy levels for charmonium hybrids in the Π_u and Σ_u^- potentials. The charm quark mass is $m_c = 1.48$ GeV. The energy offset has been chosen so that the ground-state $\Pi_u(1P)$ energy level is 4.212 GeV.

For the energy levels shown in Figs. 2 and 3, the splittings for bottomonium hybrids are less than 3/4 of those for the corresponding charmonium hybrids. The bottomonium hybrids are smaller than the corresponding charmonium hybrids. One measure of the size is the outer classical turning radius at which the potential is equal to the energy of the state. For the energy levels shown in Figs. 2 and 3, the outer classical turning radii for the bottomonium hybrids are less than 3/4 of those for the corresponding charmonium hybrids.

We can probably get better estimates for the energies of charmonium hybrids by using lattice QCD to determine the ground-state energy for each B-O configuration and using the Schroedinger equation only to calculate the differences between the energy levels nL for that B-O configuration. As the inputs to determine the ground-state energy levels $\Pi_u^+(1P)$, $\Pi_u^-(1P)$, and $\Sigma_u^-(1S)$ for charmonium hybrids, we choose the lattice QCD results for the spin-averaged energies of the H_1, H_2, and H_3 multiplets in Table VI. As the inputs to determine the ground-state energy levels $\Pi_u^+(1P)$, $\Pi_u^-(1P)$, and $\Sigma_u^-(1S)$ for bottomonium hybrids, we choose the lattice NRQCD results for the energies of the 1^{--}, 1^{++}, and 0^{++} states in Table VII. The resulting predictions for the energy levels of charmonium hybrids and bottomonium hybrids are given in Table X.

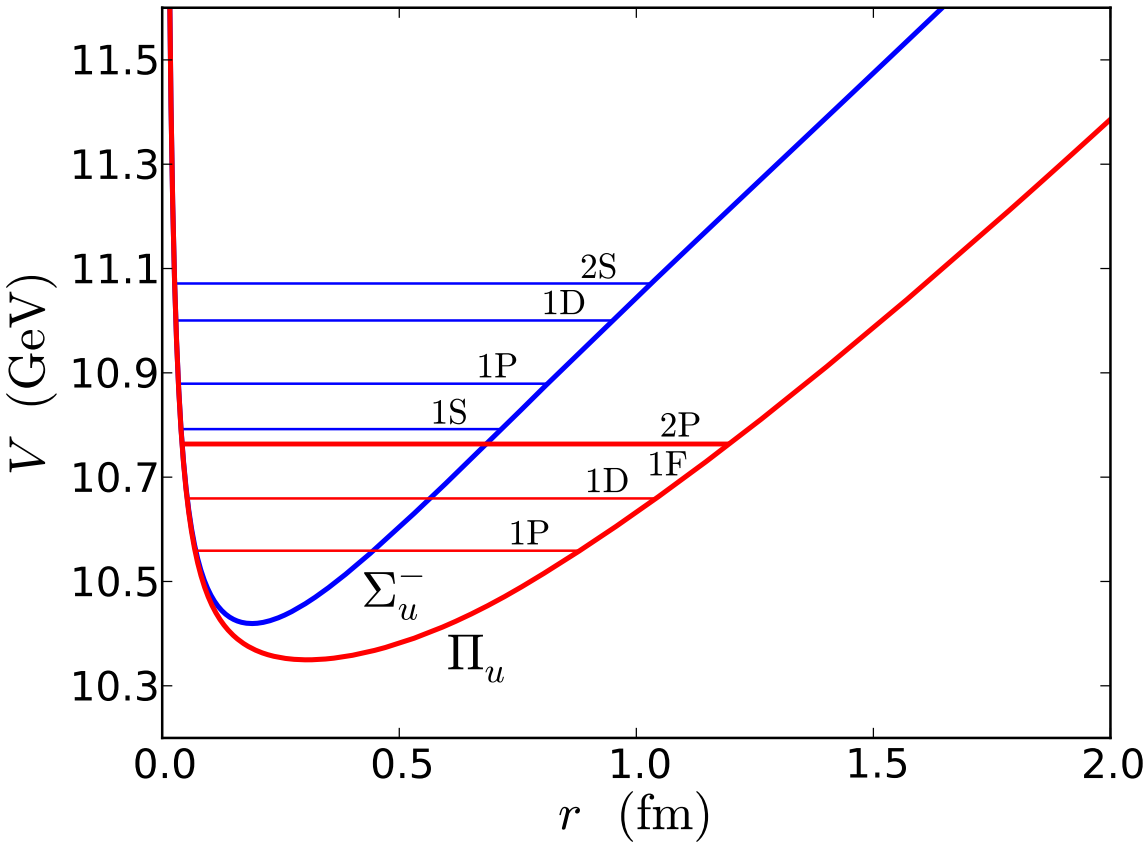

FIG. 3: Lowest energy levels for bottomonium hybrids in the Π_u and Σ_u^- potentials. The bottom quark mass is $m_b = 4.89$ GeV. The energy offset has been chosen so that the ground-state $\Pi_u(1P)$ energy level is 10.559 GeV.

C. Tetraquarks

If the tetraquark potentials were known, we could calculate the energy levels of quarkonium tetraquarks in the B-O approximation by solving the radial Schroedinger equation in Eq. (21). Unfortunately, our only information about the tetraquark potentials from QCD is that the lowest-energy adjoint mesons in quenched lattice QCD are a vector 1^- and a pseudoscalar 0^-. In Section III E, we inferred from the existence of these adjoint mesons that the deepest tetraquark B-O potentials are Π_g and Σ_g^+, which are equal at $r = 0$, and Σ_u^-. We have no information from QCD about the behavior of these potentials at nonzero r. In order to illustrate the B-O approximation for quarkonium tetraquarks, we will make the simple assumption that the tetraquark Π_g and Σ_g^+ potentials have the same shapes as the hybrid Π_u and Σ_u^- potentials, which are shown in Fig. 2. Under this assumption, the splittings between energy levels in the tetraquark Π_g potential are the same as those in the hybrid Π_u potential, and the splittings between energy levels in the tetraquark Σ_g^+ potential are the same as those in the hybrid Σ_u^- potential. The splittings in the hybrid potentials are given in Table X. If the ground-state energy level for a tetraquark B-O configuration was known, then all the higher energy levels would be determined.

multiplet	Γ	nL	$c\bar{c}$ hybrid	$b\bar{b}$ hybrid	$S=0$	$S=1$
H_1	Π_u^+	$1P$	(4212)	(10559)	1^{--}	$(0,\mathbf{1},2)^{-+}$
H_4		$1D$	4394	10659	2^{++}	$(1,\mathbf{2},3)^{+-}$
H_1'		$2P$	4562	10766	1^{--}	$(0,\mathbf{1},2)^{-+}$
H_2	Π_u^-	$1P$	(4314)	(10597)	1^{++}	$(\mathbf{0},1,\mathbf{2})^{+-}$
		$1D$	4496	10697	2^{--}	$(\mathbf{1},2,\mathbf{3})^{-+}$
		$2P$	4664	10804	1^{++}	$(\mathbf{0},1,\mathbf{2})^{+-}$
H_3	Σ_u^-	$1S$	(4407)	(10892)	0^{++}	1^{+-}
		$1P$	4544	10979	1^{--}	$(0,\mathbf{1},2)^{-+}$
		$2S$	4822	11171	0^{++}	1^{+-}

TABLE X: Energy levels (in MeV) for charmonium and bottomonium hybrids in the Π_u and Σ_u^- potentials. For each configuration Γ, the ground-state energy level in parentheses is an input. The inputs for the charmonium hybrids are the spin-averaged energies of the H_1, H_2, and H_3 multiplets from the lattice QCD results in Table VI. The inputs for the bottomonium hybrids are the energies of the 1^{--}, 1^{++}, and 0^{++} states from the lattice NRQCD results in Table VII. The energy splittings for the first orbital-angular-momentum excitation and the first radial excitation are calculated by solving the radial Schroedinger equation in the Π_u and Σ_u^- potentials. A boldfaced $\boldsymbol{J}$ indicates an exotic quantum number.

In Section IV D, selection rules for hadronic transitions were used to identify some of the XYZ mesons listed in Tables I and II with ground-state energy levels of charmonium hybrids and charmonium tetraquarks. The $Z_c^+(4020)$ and $Z_2^+(4050)$ were identified as spin-singlet and spin-triplet energy levels in the isospin-1 $\Pi_g^-(1P)$ multiplet, respectively. The $X(3915)$ and $Y(4140)$ were identified as spin-triplet states in the isospin-0 and $s\bar{s}$ $\Pi_g^-(1P)$ multiplets, respectively. Two possible identifications were proposed for both the $Z_c^+(3900)$ and $Y(4260)$. The $Z_c^+(3900)$ could be a spin-triplet state in either the isospin-1 $\Pi_g^+(1P)$ multiplet or the isospin-1 $\Sigma_g^+(1S)$ multiplet. The $Y(4260)$ could be a spin-triplet 1^{--} state in either the isospin-0 $\Pi_g^+(1P)$ multiplet or the isospin-0 $\Sigma_g^+(1S)$ multiplet. The hybrid Π_u potential is deeper than the hybrid Σ_u^- potential. If the tetraquark Π_g potential is similarly deeper than the tetraquark Σ_g^+ potential, the more plausible identifications are $Z_c^+(3900)$ as the spin-triplet state in the isospin-1 $\Pi_g^+(1P)$ multiplet and $Y(4260)$ as the spin-triplet 1^{--} state in the isospin-0 $\Sigma_g^+(1S)$ multiplet.

A speculative illustration of the spectrum of charmonium tetraquarks is given in Table XI. The masses of the $Z_c^+(4020)$, $X(3915)$, and $Y(4140)$ are used as the inputs for the $\Pi_g^-(1P)$ energy levels of the isospin-1, isospin-0, and $s\bar{s}$ tetraquarks, respectively. The mass of the $Z_c^+(3900)$ is used as the input for the $\Pi_g^+(1P)$ energy level of the isospin-1 tetraquark. The inputs for the $\Pi_g^+(1P)$ energy levels of the isospin-0 and $s\bar{s}$ tetraquarks are then obtained by assuming that the differences between the $\Pi_g^+(1P)$ and $\Pi_g^-(1P)$ energies are the same for isospin 1, isospin 0, and $s\bar{s}$. The mass of the $Y(4260)$ is used as the input for the $\Sigma_g^+(1S)$ energy level for the isospin-0 tetraquark. The inputs for the $\Sigma_g^+(1S)$ energy levels of the isospin-1 and $s\bar{s}$ tetraquarks are then obtained by assuming that the differences between the $\Sigma_g^+(1S)$ and $\Pi_g^-(1P)$ energies are the same for isospin 1, isospin 0, and $s\bar{s}$. In Table XI, the energies of the first orbital-angular-momentum excitation and the first radial excitation for each B-O configuration were obtained by assuming that their splittings from the ground

Γ	nL	isospin-1	isospin-0	$s\bar{s}$	$S=0$	$S=1$
Π_g^-	$1P$	**(4023)**	**(3918)**	**(4145)**	1^{+-}	$(0,1,2)^{++}$
	$1D$	4205	4100	4327	2^{-+}	$(1,2,3)^{++}$
	$2P$	4373	4268	4495	1^{+-}	$(0,1,2)^{++}$
Π_g^+	$1P$	**(3898)**	(3793)	(4020)	$\mathbf{1}^{-+}$	$(\mathbf{0},1,2)^{--}$
	$1D$	4080	3975	4201	$\mathbf{2}^{+-}$	$(1,2,3)^{++}$
	$2P$	4248	4143	4370	$\mathbf{1}^{-+}$	$(\mathbf{0},1,2)^{--}$
Σ_g^+	$1S$	(4368)	**(4263)**	(4490)	0^{-+}	1^{--}
	$1P$	4505	4400	4627	1^{+-}	$(0,1,2)^{++}$
	$2S$	4783	4678	4905	0^{-+}	1^{--}
Σ_u^-	$1S$				0^{++}	1^{+-}
	$1P$				1^{--}	$(0,\mathbf{1},2)^{-+}$
	$2S$				0^{++}	1^{+-}

TABLE XI: Energy levels (in MeV) for charmonium tetraquarks in the Π_g, Σ_g^+, and Σ_u^- potentials. The boldfaced experimental inputs in parentheses are the measured masses of the $Z_c^+(4020)$, $X(3915)$, $Y(4140)$, $Z_c^+(3900)$, and $Y(4260)$. The other inputs in parentheses are obtained by assuming that the splittings between ground-state energy levels are the same for isospin-1, isospin-0, and $s\bar{s}$. The energy splittings for the first orbital-angular-momentum excitation and the first radial excitation are calculated by solving the Schroedinger equation in the tetraquark Π_g and Σ_g^+ potentials under the assumption that they have the same shapes as the hybrid Π_u and Σ_u^- potentials. For an isospin-1 tetraquark, the J^{PC}'s are those of the neutral member of the isospin multiplet. A boldfaced $\boldsymbol{J}$ indicates an exotic quantum number.

state are the same as the analogous splittings for charmonium hybrids in Table X. The splittings between the Π_g^- energy levels in Table XI and those between the Π_g^+ energy levels in Table XI are the same as those between the Π_u^+ energy levels or between the Π_u^- energy levels in Table X. The splittings between the Σ_g^+ energy levels in Table XI are the same as those between the Σ_u^- energy levels in Table X. No results are given in Table XI for the energy levels in the Σ_u^- potential, because there are no XYZ mesons that are plausible candidates for any of the $\Sigma_u^-(1P)$ energy levels. The energy levels in Table XI are based on very naive assumptions about the tetraquark potentials, so they should be treated as illustrative only.

VII. OUTLOOK

The Born-Oppenheimer (B-O) approximation provides a starting point for a coherent description of all the XYZ mesons that is based firmly on QCD. The basis for the B-O approximation is that an XYZ meson contains a heavy $Q\bar{Q}$ pair, and the time scale for the evolution of the gluon and light-quark fields is small compared to that for the motion of the Q and $\bar{Q}$. The B-O approximation was first developed by Juge, Kuti, and Morningstar for flavor-singlet $Q\bar{Q}$ mesons [13], which are quarkonium and quarkonium hybrids. However, it can also be applied to flavor-nonsinglet $Q\bar{Q}$ mesons, which are quarkonium tetraquarks [11]. Most of the simple constituent models for the XYZ mesons that have been proposed can

be interpreted as different regions of the $Q\bar{Q}$ wavefunction in the B-O approximation.

The B-O approximation involves an adiabatic approximation that reduces the aspects of the problem that involve gluon and light-quark fields to the simpler problem of calculating B-O potentials, which are the energy levels of the light fields in the presence of static Q and $\bar{Q}$ sources. The B-O potentials can be calculated using lattice QCD. In order to develop quantitative phenomenology of the XYZ mesons based on the B-O approximation, it is important to have calculations of all the most relevant B-O potentials using lattice QCD with dynamical light quarks. Juge, Kuti, and Morningstar calculated many of the flavor-singlet B-O potentials using quenched lattice QCD [13]. There have been some calculations of the two deepest hybrid potentials using lattice QCD with dynamical light quarks [27, 29]. There have been no calculations of tetraquark potentials using lattice QCD, but there have been calculations of the energies of static adjoint mesons using quenched lattice QCD [32]. We have inferred the Λ_η^ϵ quantum numbers of the deepest tetraquark potentials from the J^{PC} quantum numbers of the lowest-energy static adjoint mesons. Calculations of the deepest tetraquark potentials are needed to confirm their Λ_η^ϵ quantum numbers and to determine their behavior as functions of r.

The adiabatic approximation reduces the QCD problem of determining the spectrum of $Q\bar{Q}$ mesons to a quantum mechanics problem for a $Q\bar{Q}$ pair with infinitely many coupled channels. The B-O approximation involves a further single-channel approximation that reduces the problem to a Schroedinger equation for a single radial wavefunction. This single-channel approximation may be adequate for many of the XYZ mesons. However it breaks down if the mass of the meson is too close to a threshold for a pair of heavy mesons. In this case, it is necessary to take into account the coupling to the meson-pair scattering channel. Near the meson-pair threshold, there will be an avoided crossing between a B-O potential that increases linearly at large r and one that approaches a constant equal to the meson-pair threshold. Lattice QCD calculations of B-O potentials in regions near their avoided crossings are needed in order to determine the effects of the couplings between the channels.

The B-O approximation can be used to describe hadronic transitions between XYZ mesons. The spin selection rule and the B-O selection rules provide strong constraints on the XYZ mesons that are plausible candidates for specific energy levels in the hybrid and tetraquark potentials [39]. If these potentials are calculated as functions of r, a much more detailed phenomenology of the hadronic transitions can be developed. Given an observed hadronic transition between energy levels in two B-O potentials, the rate for the same hadronic transition between any other pair of energy levels can be estimated using overlap integrals of radial wavefunctions and the group theory for angular momentum.

To understand the XYZ mesons in detail, it will be necessary to develop a framework in which corrections to the B-O approximation can be calculated systematically. There is an effective field theory for the $Q\bar{Q}$ sector of QCD called potential NRQCD in which the QCD interactions are reduced to interaction potentials between the Q and $\bar{Q}$ and multipole couplings of the $Q\bar{Q}$ pair to soft gluons [30]. Unfortunately, this effective field theory seems to be applicable only to the most deeply bound quarkonium states and perhaps only to the ground-state bottomonium states $\Upsilon(1S)$ and $\eta_b(1S)$. The development of an effective field theory in which the adiabatic approximation emerges as a first approximation would provide a powerful framework for describing the XYZ mesons.

The B-O approximation predicts that the observed XYZ mesons are only the tip of an iceberg. There are many more XYZ mesons waiting to be discovered. The selection rules for

hadronic transitions can provide some guidance for searches for additional XYZ mesons. New XYZ mesons could be discovered in existing data from the B-factory experiments Belle and Babar and from the LHC experiments ATLAS, CMS, and LHCb. The BESII collaboration is continuing to discover additional $c\bar{c}$ XYZ mesons at BEPC-II. Even more XYZ mesons should be discovered at the upcoming higher-luminosity B factory SuperBelle and at the upcoming higher-luminosity runs of the LHC. Precision measurements of some of the properties of XYZ mesons should be possible at both SuperBelle and eventually at the PANDA detector at GSI. All this additional data will make the elucidation of the nature of the XYZ mesons almost inevitable. It will deliver a definitive verdict on whether the Born-Oppenheimer approximation provides a coherent theoretical framework for understanding the XYZ mesons.

Acknowledgments

This research was supported in part by the Department of Energy under grant DE-FG02-05ER15715 and by the National Science Foundation under grant PHY-1310862.

[1] S. K. Choi *et al.* [Belle Collaboration], Phys. Rev. Lett. **91**, 262001 (2003) [hep-ex/0309032].
[2] B. Aubert *et al.* [BaBar Collaboration], Phys. Rev. Lett. **95**, 142001 (2005) [hep-ex/0506081].
[3] T. Aaltonen *et al.* [CDF Collaboration], Phys. Rev. Lett. **102**, 242002 (2009) [arXiv:0903.2229].
[4] A. Bondar *et al.* [Belle Collaboration], Phys. Rev. Lett. **108**, 122001 (2012) [arXiv:1110.2251].
[5] M. Ablikim *et al.* [BESIII Collaboration], Phys. Rev. Lett. **110**, 252001 (2013) [arXiv:1303.5949].
[6] G. T. Bodwin, E. Braaten, E. Eichten, S. L. Olsen, T. K. Pedlar and J. Russ, arXiv:1307.7425 [hep-ph].
[7] J. Vijande, E. Weissman, A. Valcarce and N. Barnea, Phys. Rev. D **76** (2007) 094027 [arXiv:0710.2516].
[8] N. A. Tornqvist, Z. Phys. C **61** (1994) 525 [hep-ph/9310247].
[9] N. Drenska, R. Faccini, F. Piccinini, A. Polosa, F. Renga and C. Sabelli, Riv. Nuovo Cim. **033** (2010) 633 [arXiv:1006.2741].
[10] S. Dubynskiy and M. B. Voloshin, Phys. Lett. B **666** (2008) 344 [arXiv:0803.2224].
[11] E. Braaten, Phys. Rev. Lett. **111**, 162003 (2013) [arXiv:1305.6905].
[12] M. Born and J.R. Oppenheimer, Annalen der Physik **389**, 457 (1927).
[13] K.J. Juge, J. Kuti and C.J. Morningstar, Phys. Rev. Lett. **82**, 4400 (1999) [hep-ph/9902336].
[14] C. -Z. Yuan, arXiv:1312.6399 [hep-ex].
[15] Z. Q. Liu *et al.* [Belle Collaboration], Phys. Rev. Lett. **110**, 252002 (2013) [arXiv:1304.0121].
[16] K. Chilikin *et al.* [Belle Collaboration], Phys. Rev. D **88**, 074026 (2013) [arXiv:1306.4894].
[17] M. Ablikim *et al.* [BESIII Collaboration], Phys. Rev. Lett. **112**, 022001 (2014) [arXiv:1310.1163].
[18] M. Ablikim *et al.* [BESIII Collaboration], Phys. Rev. Lett. **111**, 242001 (2013) [arXiv:1309.1896].
[19] M. Ablikim *et al.* [BESIII Collaboration], arXiv:1308.2760 [hep-ex].
[20] T. Xiao, S. Dobbs, A. Tomaradze and K.K. Seth, arXiv:1304.3036 [hep-ex].

[21] I. Adachi *et al.* [Belle Collaboration], arXiv:1209.6450 [hep-ex].
[22] I. Adachi *et al.* [Belle Collaboration], arXiv:1207.4345 [hep-ex].
[23] K. J. Juge, J. Kuti and C. Morningstar, Phys. Rev. Lett. **90**, 161601 (2003) [hep-lat/0207004].
[24] E. Eichten, K. Gottfried, T. Kinoshita, J. B. Kogut, K. D. Lane and T. -M. Yan, Phys. Rev. Lett. **34**, 369 (1975) [Erratum-ibid. **36**, 1276 (1976)].
[25] R. Sommer, Nucl. Phys. B **411**, 839 (1994) [hep-lat/9310022].
[26] G.S. Bali, Phys. Rept. **343**, 1 (2001) [hep-ph/0001312].
[27] G. S. Bali *et al.* [TXL and T(X)L Collaborations], Phys. Rev. D **62**, 054503 (2000) [hep-lat/0003012].
[28] B. Bolder, T. Struckmann, G. S. Bali, N. Eicker, T. Lippert, B. Orth, K. Schilling and P. Ueberholz, Phys. Rev. D **63**, 074504 (2001) [hep-lat/0005018].
[29] G. S. Bali *et al.* [SESAM Collaboration], Phys. Rev. D **71**, 114513 (2005) [hep-lat/0505012].
[30] N. Brambilla, A. Pineda, J. Soto and A. Vairo, Nucl. Phys. B **566**, 275 (2000) [hep-ph/9907240].
[31] N. A. Campbell, I. H. Jorysz and C. Michael, Phys. Lett. B **167**, 91 (1986).
[32] M. Foster *et al.* [UKQCD Collaboration], Phys. Rev. D **59**, 094509 (1999) [hep-lat/9811010].
[33] K. Marsh and R. Lewis, Phys. Rev. D **89**, 014502 (2014) [arXiv:1309.1627].
[34] A. Vairo, arXiv:0912.4422 [hep-ph].
[35] G. S. Bali and A. Pineda, Phys. Rev. D **69**, 094001 (2004) [hep-ph/0310130].
[36] A.E. Bondar, A. Garmash, A.I. Milstein, R. Mizuk and M.B. Voloshin, Phys. Rev. D **84**, 054010 (2011) [arXiv:1105.4473].
[37] M. Cleven, F.-K. Guo, C. Hanhart and Ulf-G. Meissner, Eur. Phys. J. A **47**, 120 (2011) [arXiv:1107.0254].
[38] T. Mehen and J.W. Powell, Phys. Rev. D **84**, 114013 (2011) [arXiv:1109.3479].
[39] E. Braaten, C. Langmack and D. H. Smith, arXiv:1401.7351 [hep-ph].
[40] J. P. Lees *et al.* [BaBar Collaboration], Phys. Rev. D **86**, 072002 (2012) [arXiv:1207.2651 [hep-ex]].
[41] R. Mizuk *et al.* [Belle Collaboration], Phys. Rev. D **78**, 072004 (2008) [arXiv:0806.4098].
[42] I. Adachi *et al.* [Belle Collaboration], arXiv:0808.2445 [hep-ex].
[43] J. J. Dudek, R. G. Edwards, N. Mathur and D. G. Richards, Phys. Rev. D **77**, 034501 (2008) [arXiv:0707.4162].
[44] L. Liu *et al.* [Hadron Spectrum Collaboration], JHEP **1207**, 126 (2012) [arXiv:1204.5425].
[45] J.J. Dudek, Phys. Rev. D **84**, 074023 (2011) [arXiv:1106.5515].
[46] G. P. Lepage, L. Magnea, C. Nakhleh, U. Magnea and K. Hornbostel, Phys. Rev. D **46**, 4052 (1992) [hep-lat/9205007].
[47] X. Liao and T. Manke, Phys. Rev. D **65**, 074508 (2002) [hep-lat/0111049].
[48] S. Prelovsek and L. Leskovec, Phys. Lett. B **727**, 172 (2013) [arXiv:1308.2097].
[49] W. Chen, R. T. Kleiv, T. G. Steele, B. Bulthuis, D. Harnett, J. Ho, T. Richards and S. -L. Zhu, JHEP 2013:19 [arXiv:1304.4522].
[50] J. Beringer *et al.* [Particle Data Group Collaboration], Phys. Rev. D **86**, 010001 (2012).